Entanglement dynamics in Heisenberg spin chains coupled to a dissipative environment at finite temperature

Gehad Sadiek[1,2,*] and Samaher Almalki[3]
[1]*Department of Applied Physics and Astronomy, University of Sharjah, Sharjah 27272, UAE*
[2]*Department of Physics, Ain Shams University, Cairo 11566, Egypt*
[3]*Department of Physics, King Saud University, Riyadh 11451, Saudi Arabia*
(Received 7 April 2016; published 25 July 2016)

We consider a finite one-dimensional Heisenberg *XYZ* spin chain under the influence of a dissipative Lindblad environment obeying the Born-Markovian constraint in presence of an external magnetic field with closed and open boundary conditions. We present an exact numerical solution for the Lindblad master equation of the system in the Liouville space. The dynamics and asymptotic behavior of the nearest-neighbor and beyond-nearest-neighbor pairwise entanglements in the system are investigated under the effect of spatial anisotropy, temperature, system size, and different initial states. The entanglements in the free spin system exhibit nonuniform oscillatory behavior that varies significantly depending on the system size, anisotropy, and initial state. The xy spatial anisotropy dictates the asymptotic behavior of the different entanglements in the system under the influence of the environment regardless of the initial state. Higher anisotropy yields higher steady-state value of the nearest-neighbor entanglement whereas a complete isotropy wipes it out. The longer range entanglements respond differently to the anisotropy variation. The anisotropy in the z direction may enhance the entanglements depending on the interplay with the magnetic field applied in the same direction. As the temperature is raised, the steady state of the short-range entanglements is found to be robust within very small nonzero temperature range that depends critically on the spatial anisotropy. Moreover, the end to end entanglement transfer time and speed through the open boundary chain vary considerably based on the degree of anisotropy and temperature of the environment.

DOI: 10.1103/PhysRevA.94.012341

I. INTRODUCTION

Quantum entanglement plays a vital role in the static and dynamic behavior of many-body systems [1]. It is considered as the physical resource responsible for manipulating the linear superposition of the quantum states in quantum systems. Entanglement, and its derivatives, show scaling behavior as the physical system experiences a quantum phase transition [2]. Particularly, it is considered as a crucial resource in quantum information processing fields such as quantum teleportation, cryptography, and quantum computation where it provides the physical basis for implementing the different needed algorithms [3]. Therefore, creating, quantifying, transferring, and protecting entanglement in quantum states of multiparticle systems are the focus of interest of both theoretical and experimental research. However, quantum entanglement is very fragile due to the induced decoherence caused by the inevitable coupling of the quantum system to its surrounding environment [4,5]. The main effect of decoherence is to randomize the relative coherent phases of the possible states of the quantum system diminishing its quantum aspects. It is considered as one of the main obstacles toward realizing an effective quantum computing system. Offering a potentially ideal protection against environmentally induced decoherence is found to be a very difficult task. The decoherence in the system causes sweeping out of entanglement between the different parties of the system. Therefore, monitoring the entanglement dynamics in the considered system helps us understand the behavior of the decoherence as well.

The Heisenberg interacting spin systems have been a focus of interest for their own sake as they describe the novel physics of localized spins in magnetic systems as well as for their successful role in representing many of the physical systems that are very promising candidates for quantum information processing such as the solid-state systems [6–8], NMR [9,10], optical lattices [11,12], electronic spins [13], and superconducting arrays [14]. Entanglement properties and dynamics in Heisenberg spin chains in the absence of dissipative environments have been studied intensively [15–22]. There have been several interesting works that focused on the dynamics of a system of interacting qubits, represented by the Heisenberg spin model, coupled to dissipative environments. Particularly, the problem of two qubits coupled to dissipative environments has been intensively studied. Analytic and numerical solutions were provided for a two-qubit XY system in an external magnetic field coupled to a population relaxation environment as well as a thermal environment [23]. It was shown that the system reaches a steady-state value though it is coupled to a population relaxation environment, which causes decoherence, provided that the spatial anisotropy of the system is maintained. The steady-state value may vanish as the temperature of the thermal environment is raised. The anisotropic two-qubit *XYZ* Heisenberg model in an inhomogeneous magnetic field coupled to a population relaxation environment at zero temperature was investigated too, both analytically and numerically [24]. It was demonstrated that the two-qubit system reaches a steady state starting from an initial separable state as long as the anisotropy of the spin coupling in the x and y direction is nonzero regardless of the value of the coupling in the z direction. The spin relaxation in a two-qubit Ising system under a single spin-flip inducing

*Corresponding author: gsadiek@sharjah.ac.ae

environment was investigated and the relaxation rates were calculated [25].

The one-dimensional multiqubit chains, $N > 2$, coupled to dissipative environments were investigated as well at different degrees of anisotropy, magnetic-field strength, and temperatures [26–33]. Of most relevance, the time evolution of the concurrence of the nearest-neighbor spins in a one-dimensional XX spin chain in the absence of any external magnetic fields coupled to thermal and dephasing environments were studied [29]. It was shown that in all cases the entanglement vanishes within a finite time that depends on the system-environment coupling parameter and temperature. The dynamics of entanglement in the Ising and isotropic (XXX) one-dimensional spin chains has been investigated [28] using the numerical stochastic approach by applying the quantum state diffusion theory [34], which reduces the needed huge storage space from 2^{2N} to 2^N for N interacting spins. They focused on the influence of noise during short periods of time. The effect of the initial state of the system on the time evolution behavior under coupling with the environment was considered and it was shown that most of the time the main effect of the noise is to reduce the amplitude of the large oscillation of the entanglement. An Ising one-dimensional spin system in an external magnetic field with two nonvanishing components in the x and z directions and coupled to a Markovian environment was investigated using stochastic calculations too [31]. One particular work of special interest considered a one-dimensional chain of superconducting Josephson qubits with experimentally realistic conditions [27]. The effect of the environmental noise on the entanglement in the chain was tested. The influence of the noise was introduced as a set of bosonic baths such that each one of them is coupled to a single qubit. It was shown that this noise environment causes a significant change to the entanglement dynamics of the Josephson qubits. In the limiting case when the internal degrees of freedom of the baths were traced out the system behaves as an Ising spin chain coupled to a Born-Markovian environment with an asymptotic steady-state entanglement. Other recent works have investigated the entanglement dynamics in spin systems under different environmental and external effects and focused on the entanglement and information transfer through the system [35–38].

In this paper, we investigate the time evolution and transfer of quantum entanglement in a finite one-dimensional Heisenberg XYZ spin-1/2 chain with nearest-neighbor spin interaction under the influence of dissipative Lindblad environment in presence of an external magnetic field at zero and finite temperature. We consider both cases of closed and open boundary spin chains with maximum number of seven spins. We provide an exact numerical solution of the Lindblad master equation of the system. In the closed boundary case, we show how the nearest-neighbor (nn) and beyond-nearest-neighbor entanglement (nnn, nnnn,...) as well as the one-tangle τ_1 and the overall bipartite entanglement τ_2 in the free (isolated) system evolve in time in a nonuniform oscillatory form that changes significantly depending on the initial state of the system, the number of spins, and the degree of spatial anisotropy but disappears in the presence of the environment. Also, we investigate the asymptotic steady state of the entanglement at the different ranges in the system under the influence of the environment at zero temperature and show how it varies strongly and differently based on the degrees of anisotropy of the spin coupling strength, leading to either a vanishing or a constant steady-state value. We emphasize the important role played by the interplay between the spin coupling in the z direction and the external magnetic field applied in the z direction. We explore the robustness of the quantum effects and the steady state of the entanglement at finite temperature and its critical dependence on the degree of anisotropy. We study the end to end entanglement transfer through the open boundary chain starting from an initial state with a maximum entanglement at one terminal of the chain and disentanglement over the rest of it. We discuss how the entanglement transfer time, speed, and residue through the chain vary depending on the degrees of anisotropy, the temperature, and the separation from the maximally entangled end. This paper is organized as follows. In the next section, we present our model and calculations. In Sec. III, we study the time evolution of the entanglement in Heisenberg spin chains with closed boundary condition in the absence and presence of the Lindblad environment at zero and finite temperature. In Sec. IV, we investigate the entanglement transfer in a Heisenberg chain with open boundary condition under the influence of thermal and dissipative environments. We conclude in Sec. V.

II. MODEL

We consider a one-dimensional system of N spin-1/2 particles with nearest-neighbor coupling J in an external magnetic field in the z direction B. The system is described by the Heisenberg Hamiltonian

$$H = \frac{(1+\gamma)}{2} J \sum_{i=1}^{N} S_i^x S_{i+1}^x + \frac{(1-\gamma)}{2} J \sum_{i=1}^{N} S_i^y S_{i+1}^y + \delta J \sum_{i=1}^{N} S_i^z S_{i+1}^z + \sum_{i=1}^{N} B^z S_i^z, \quad (1)$$

where $S_i^\alpha = \frac{1}{2}\sigma_i^\alpha$ ($\alpha = x$, y, or z) and σ_i^α are the local spin-$\frac{1}{2}$ operators and Pauli operators, respectively (for convenience we set $\hbar = k = 1$). When we apply the periodic boundary condition we set $S_{N+1} = S_1$. γ and δ are the anisotropy parameters which determine the relative strength of the spin coupling in the x, y, and z directions. We study different classes of the Heisenberg spin system by changing the values of the parameters γ and δ such as the Ising ($\gamma = 1$ and $\delta = 0$), XX ($\gamma = 0$ and $\delta = 0$), XXX ($\gamma = 0$ and $\delta = 0.5$), XYZ ($\gamma = 0.5$ and $\delta = 0.5$), etc. The system is subject to an external homogeneous static magnetic field $B = B^z\,\hat{z} = \omega\,\hat{z}$ in the z direction, where ω represents the magnitude of effective applied external magnetic field as well as the energy gap of each spin.

The dynamics of an isolated quantum system is described by the time evolution of its density matrix $\rho(t)$ according to the Liouville equation $\dot{\rho}(t) = -i[H,\rho]$. But for an open quantum system that is interacting with its environment, the Liouville equation has to be modified to account for the dissipative effects of the environment on the system. If the system and the environment satisfy the conditions of weak coupling as well as short relaxation time within the environment excitation

modes, the Born-Markovian approximation can be applied and the time evolution of the system is best described by the Lindblad master equation [39,40], which preserves the Hermiticity and unit trace of the density matrix and guarantees positive continuous evolution of the system under the effect of the environment, defined by

$$\dot{\rho}(t) = -i[H,\rho] + \mathcal{D}_\rho, \tag{2}$$

where $\mathcal{D}_\rho$ is the extra term that describes the dissipative dynamics and is represented in the Lindblad form as

$$\mathcal{D}_\rho = -\frac{1}{2}\sum_{k=1}\{[L_k\rho,L_k^\dagger] + [L_k,\rho L_k^\dagger]\}, \tag{3}$$

where the Lindblad operator L_k represents all the effects of the considered environment on the system site k, where the environment is assumed to couple to each site independently of the other sites and therefore is represented by

$$L_k = \mathbf{1}_1 \otimes \mathbf{1}_2 \otimes \cdots \otimes L_k \otimes \cdots \otimes \mathbf{1}_N. \tag{4}$$

For Q- dimensional Hilbert space, the density operator is represented by a Q by Q matrix, but it is more convenient to work in the Liouville space, where it is represented as a vector with Q^2 elements, $\vec{\rho} = (\rho_{11},\rho_{12},\rho_{13},\ldots,\rho_{1Q},\ldots,\rho_{21},\rho_{22},\ldots,\rho_{2Q},\ldots,\rho_{QQ})$. In fact, the selected order of the elements is not important but has to be preserved once chosen. The main idea here is to reformulate Eq. (2) to take the matrix equation form

$$\dot{\vec{\rho}}(t) = (\hat{\mathcal{L}}^H + \hat{\mathcal{L}}^D)\vec{\rho} = \hat{\mathcal{L}}\vec{\rho}, \tag{5}$$

where $\hat{\mathcal{L}}^H$ and $\hat{\mathcal{L}}^D$ are superoperators acting on the vector ρ in the Liouville space, where the first one represents the unitary evolution due to the free Hamiltonian while the second represents the dissipation process. The matrix elements of $\dot{\rho}$ are defined as

$$\dot{\rho}_{jl}(t) = -i\sum_{m,n}\left(\mathcal{L}^H_{jl,mn} + \mathcal{L}^D_{jl,mn}\right)\ \rho_{mn}, \tag{6}$$

where the tetrahedral matrices $\mathcal{L}^H$ and $\mathcal{L}^D$ are given by

$$\mathcal{L}^H_{jl,mn} = H_{jm}\delta_{ln} - \delta_{jm}H_{nl}, \tag{7}$$

and

$$\mathcal{L}^D_{jl,mn} = \frac{i}{2}\sum_k [2(L_k^\dagger)_{nl}(L_k)_{jm} - (L_k^\dagger L_k)_{jm}\delta_{ln} - \delta_{jm}(L_k^\dagger L_k)_{nl}]. \tag{8}$$

Now the whole problem of evaluating the time evolution of the density matrix has been reduced to seeking the solution of the standard matrix equation (5) which can be achieved once we find the set of all eigenvalues $\{\lambda_1,\lambda_2,\lambda_3,\ldots,\lambda_{Q^2}\}$ and eigenvectors $\{\vec{\eta}_1,\vec{\eta}_2,\vec{\eta}_3,\ldots,\vec{\eta}_{Q^2}\}$ of the $Q^2\times Q^2$ tetrahedral matrix $\mathcal{L}$, and as a result the density vector becomes

$$\vec{\rho}(t) = \sum_{i=1}^{Q^2} A_i\ \vec{\eta}_i\ e^{\lambda_i t}, \tag{9}$$

where the coefficients A_i are determined from the initial conditions of the evolution process. Once the density (vector) matrix has been calculated as a function of time, we can evaluate the entanglement in the chain as explained below.

For a one-dimensional chain with N spin-1/2 particles, the dimension of the Hilbert space is 2^N and the dimension of the tetrahedral matrices is 2^{2N} which, even for a small number of spins, is extremely large and requires a huge computational storage that is more than what can be handled by most of the available computing systems and represents a real challenge in such type of problems.

For the Heisenberg spin chain described by the Hamiltonian (1), the effect of the dissipative and thermal environment is given by the local Lindblad operator [27,40,41]

$$L_k = \Gamma\left\{\frac{(\bar{n}+1)}{2}\ S_k^- + \bar{n}\ S_k^\dagger\right\}, \tag{10}$$

where S^+ and S^- are the spin raising and lowering operators, $S^\pm = S^x\ \pm\ iS^y$. Γ is a phenomenological parameter that determines the strength of the coupling between the environment and the system and is assumed to be the same for all spins. The thermal parameter $\bar{n}$ is proportional to the temperature of the environment. Obviously, in Eq. (10), the first term induces the dissipation process whereas the second one causes excitation. As mentioned before, for Eq. (2) to represent a good approximation for the time evolution of the system, certain restrictions have to apply to the system parameters, the coupling parameter between the system, and the environment Γ as well as the relaxation time scale of the environment dynamics should be small compared to that of the system dynamics manifested by the parameter ω representing the spin precession frequency around the z axis. As a result, we consider values of Γ and J such that Γ and $J \ll \omega$.

We adopt the concurrence as a measure of the bipartite entanglement in the system, where Wootters [42] has shown that for a pair of two-state systems i and j, the concurrence $C_{i,j}$, which varies between 0 to 1, can be used to quantify the entanglement between them and is defined by

$$C_{i,j}(\rho_{i,j}) = \max\{0,\epsilon_1 - \epsilon_2 - \epsilon_3 - \epsilon_4\}, \tag{11}$$

where $\rho_{i,j}$ is the reduced density matrix of the two spins under consideration, ϵ_i's are the eigenvalues of the Hermitian matrix $R \equiv \sqrt{\sqrt{\rho_{i,j}}\tilde{\rho_{i,j}}\sqrt{\rho_{i,j}}}$ with $\tilde{\rho_{i,j}} = (\sigma^y\otimes\sigma^y)\rho^*_{i,j}(\sigma^y\otimes\sigma^y)$, and σ^y is the Pauli matrix of the spin in the y direction.

In addition to the concurrence, which quantifies the entanglement between any two spins in the system in a pure or mixed state, it is very insightful to evaluate and study two other measures of entanglement, τ_1 and τ_2. The one-tangle $\tau_1 = 4\det\rho_1$ is a measure of the multipartite entanglement in pure states of quantum systems, where ρ_1 is the single-site reduced density matrix. It quantifies the entanglement between a single spin and the rest of the entire system. On the other hand, τ_2 is a measure of the global pairwise entanglement in the system and is defined as the sum of the squared pairwise concurrences, between a single spin, for instance i, and every other spin in the system, $\sum_{j\neq i} C^2_{i,j}$ [43,44]. The ratio $R = \tau_2/\tau_1 \leqslant 1$ was introduced as a measure of the fraction of the total entanglement attributed to the pairwise correlations within the system [45]. Therefore, the behavior of the three quantities τ_1, τ_2, and R may provide very crucial information about the system state such as factorization ($\tau_1 = \tau_2 = 0$), vanishing of bipartite entanglement in the presence of multipartite entanglement

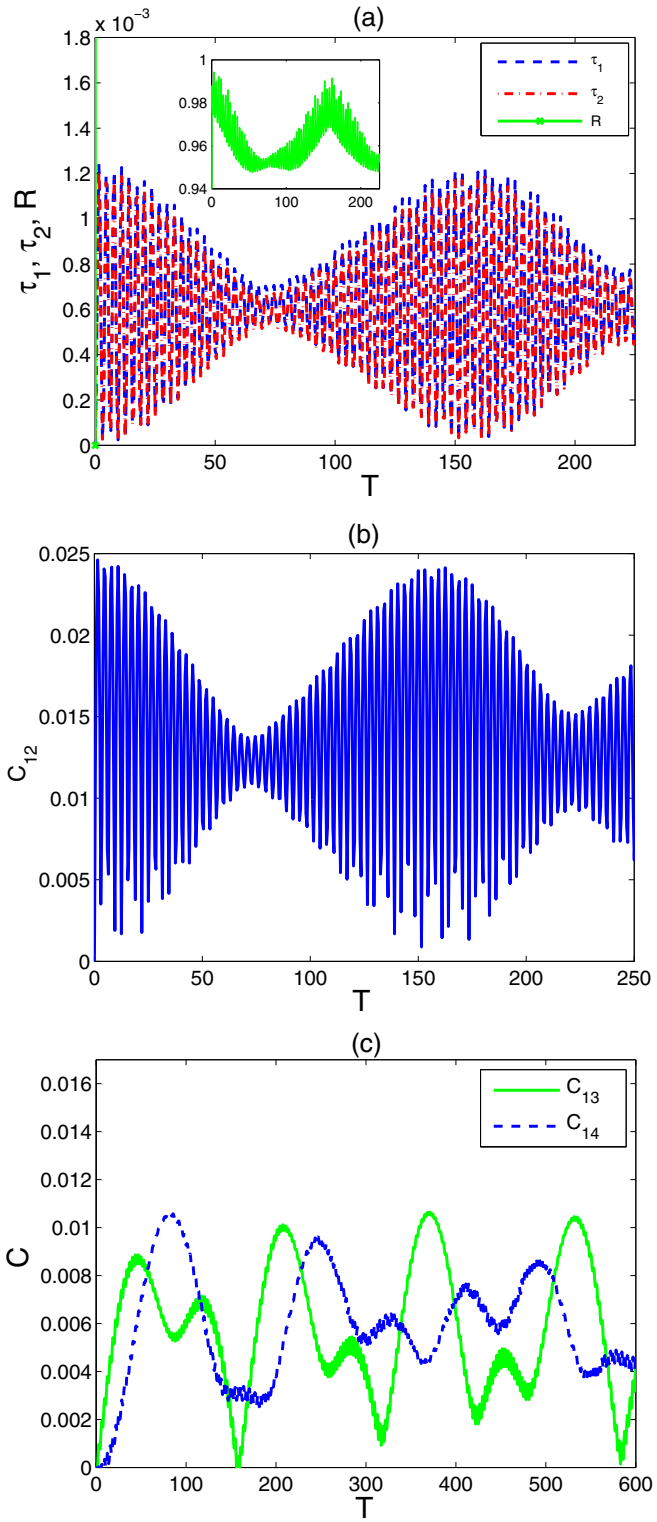

FIG. 1. Time evolution of (a) τ_1, τ_2, and R, (b) C_{12}, (c) C_{13} and C_{14} in the free ($\Gamma = 0$) Ising system starting from an initially disentangled state, where $N = 7$.

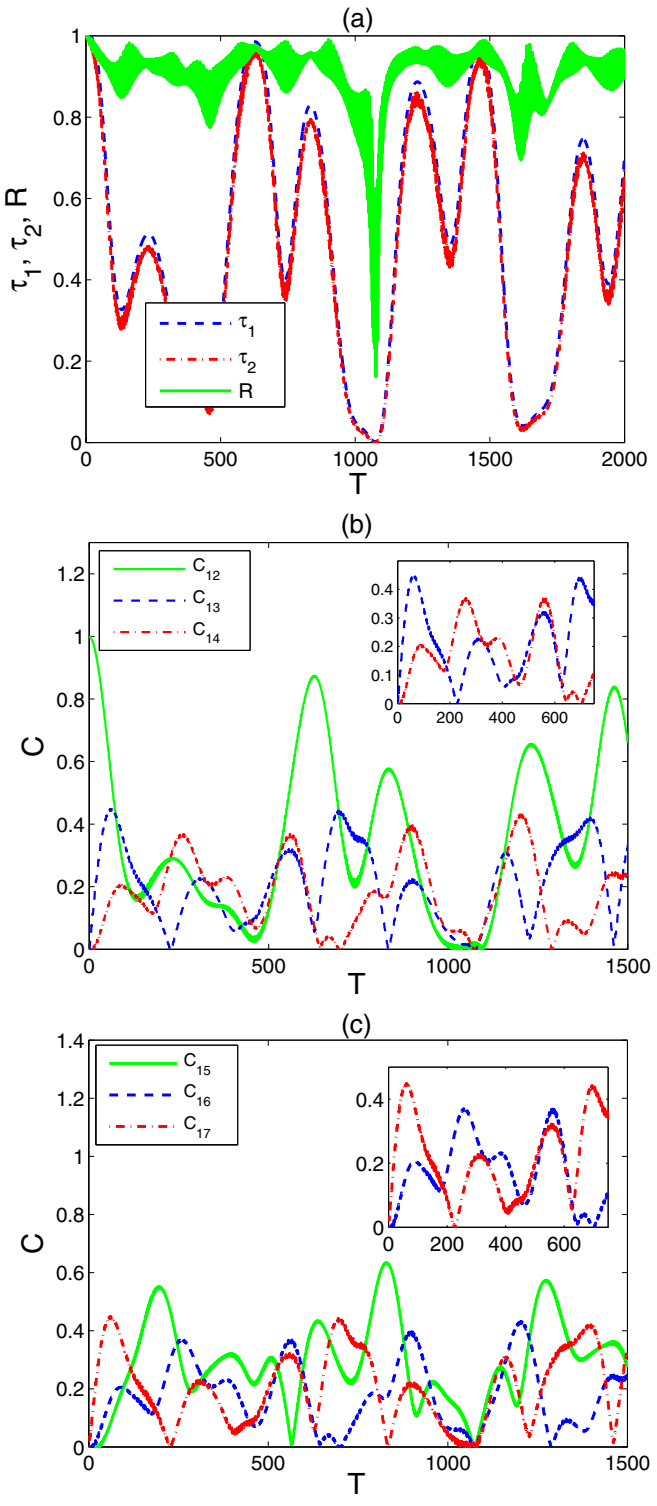

FIG. 2. Time evolution of (a) τ_1, τ_2, and R, (b) C_{12}, C_{13}, and C_{14}, (c) C_{15}, C_{16}, and C_{17} in the free ($\Gamma = 0$) Ising system starting from an initial maximally entangled state, where $N = 7$.

($\tau_2 = 0$, $\tau_1 \neq 0$), or quantum phase transitions (anomalous behavior of R). We study the dynamics of these different quantities in the free Heisenberg system. Although τ_1 and R are not defined for mixed states of the system, in the presence of the environment, yet it is very useful to evaluate τ_2. Studying the behavior of τ_2 and comparing it with that of the nearest-neighbor bipartite entanglement C_{12} provides not only information about the global pairwise entanglement in the system but also how the beyond nearest-neighbor entanglements are behaving. There are cases where C_{12} may vanish whereas τ_2 assumes a finite value. We study

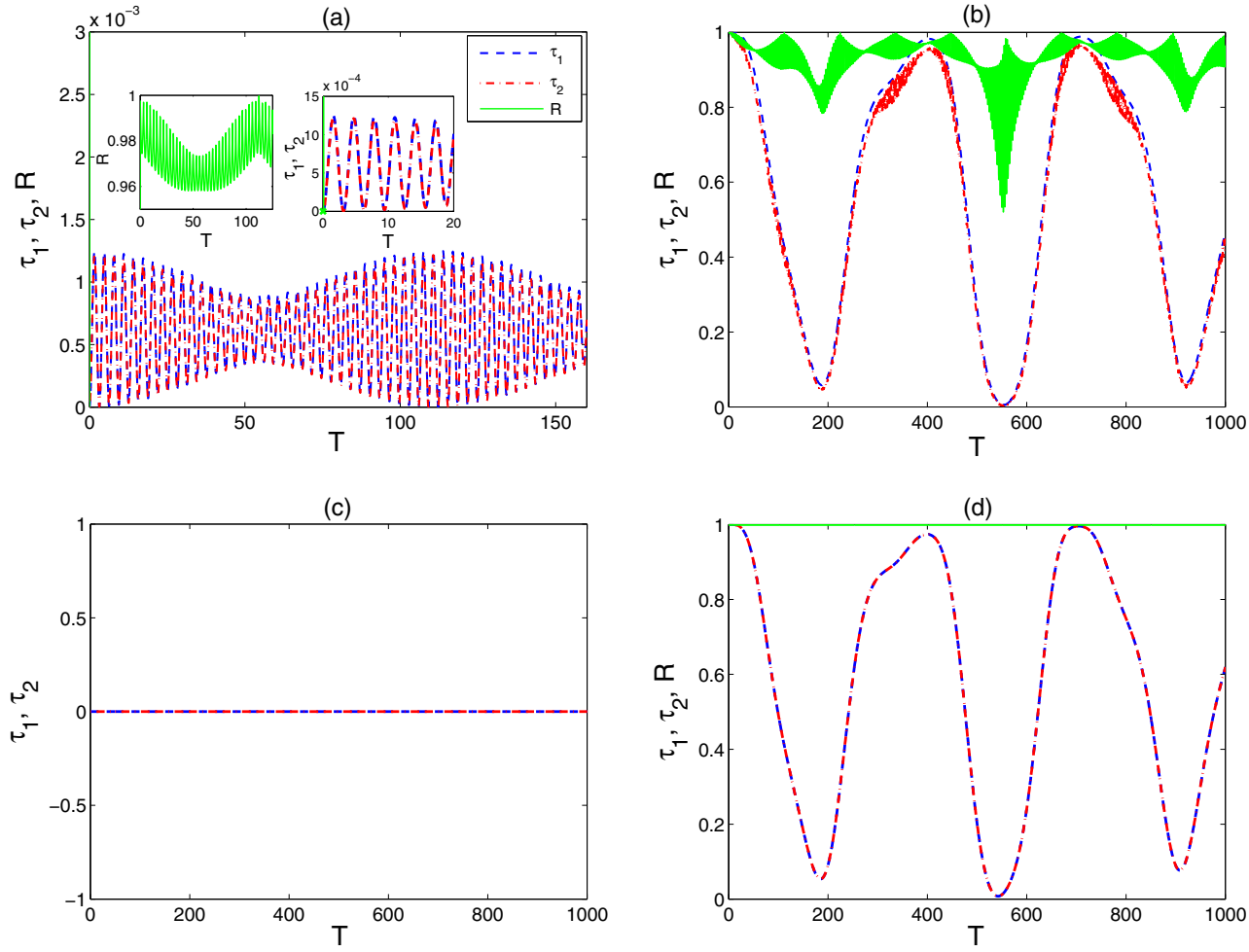

FIG. 3. Time evolution of the free Ising system ($\Gamma = 0$) starting from an initial (a) disentangled state; (b) maximally entangled state; and the free *XX* system starting from an initial (c) disentangled state; (d) maximally entangled state, where $N = 5$. The legend is as shown in panel (a).

the time evolution of the system using the standard basis $\{|\uparrow\uparrow\cdots\uparrow\rangle, |\uparrow\uparrow\cdots\downarrow\rangle, \ldots, |\uparrow\downarrow\cdots\downarrow\rangle, \ldots, |\downarrow\downarrow\cdots\downarrow\rangle\}$ and starting from different initial typical states: a separable (disentangled) state, $|\psi_s\rangle = |\uparrow\uparrow\cdots\uparrow\rangle$; a partially entangled (W state), $|\psi_w\rangle = \frac{1}{\sqrt{N}}(|\uparrow\downarrow\cdots\downarrow\rangle + |\downarrow\uparrow\cdots\downarrow\rangle + \cdots + |\downarrow\downarrow\cdots\uparrow\rangle)$, and a maximally entangled state, $|\psi_m\rangle = \frac{1}{\sqrt{2}}(|\uparrow\downarrow\rangle + |\downarrow\uparrow\rangle)|\downarrow\downarrow\cdots\downarrow\rangle$.

III. DYNAMICS OF ENTANGLEMENT IN CLOSED BOUNDARY SPIN CHAINS

A. Free system

It is very enlightening to start our study by considering the entanglement dynamics in the free (isolated) Heisenberg spin chains before considering the environment effect, which is described by the Hamiltonian (1). In general, for convenience we consider the time evolution of the system in terms of the dimensionless time $T = \omega t$. In Fig. 1, we depict the time evolution of the entanglement in the closed boundary seven-spins free Ising system starting from a completely disentangled (separable) state. The one tangle τ_1 and the overall bipartite entanglement τ_2 between spin 1 and the rest of the chain is illustrated in Fig. 1(a), where they show beatlike oscillatory behavior with very close magnitudes compared to each other and this is why their ratio $R = \tau_2/\tau_1$ is limited between about 0.95 and 0.99 as can be seen in the inner panel of the figure. This indicates that the entanglement in the system is mainly of a pairwise nature. The time evolution of the bipartite entanglement C_{12} is very similar to that of τ_1 and τ_2 but with a bigger amplitude as expected as shown in Fig. 1(b). The time evolution of the longer range entanglements C_{13} and C_{14} are illustrated in Fig. 1(c), where they show a simple nonuniform oscillatory behavior with about half the amplitude of C_{12}. The entanglements C_{15}, C_{16}, and C_{17} were found to show the same exact behavior of C_{14}, C_{13}, and C_{12} respectively as expected in a closed boundary chain. The great resemblance between the behavior of τ_1, τ_2, and C_{12} is caused by the fact that C_{12} is the main contributor to τ_2 and τ_1 is mainly of a pairwise nature ($R \approx 1$). The closed boundary free Ising chain starting from a maximally entangled state is considered in Fig. 2, where it shows a different behavior from the previous case. The entanglement functions τ_1 and τ_2 show sustainable nonuniform oscillatory behavior, with no beating, that is very close for the two except when their magnitudes decrease significantly and their ratio R changes over wider range between about 0.2 and 1

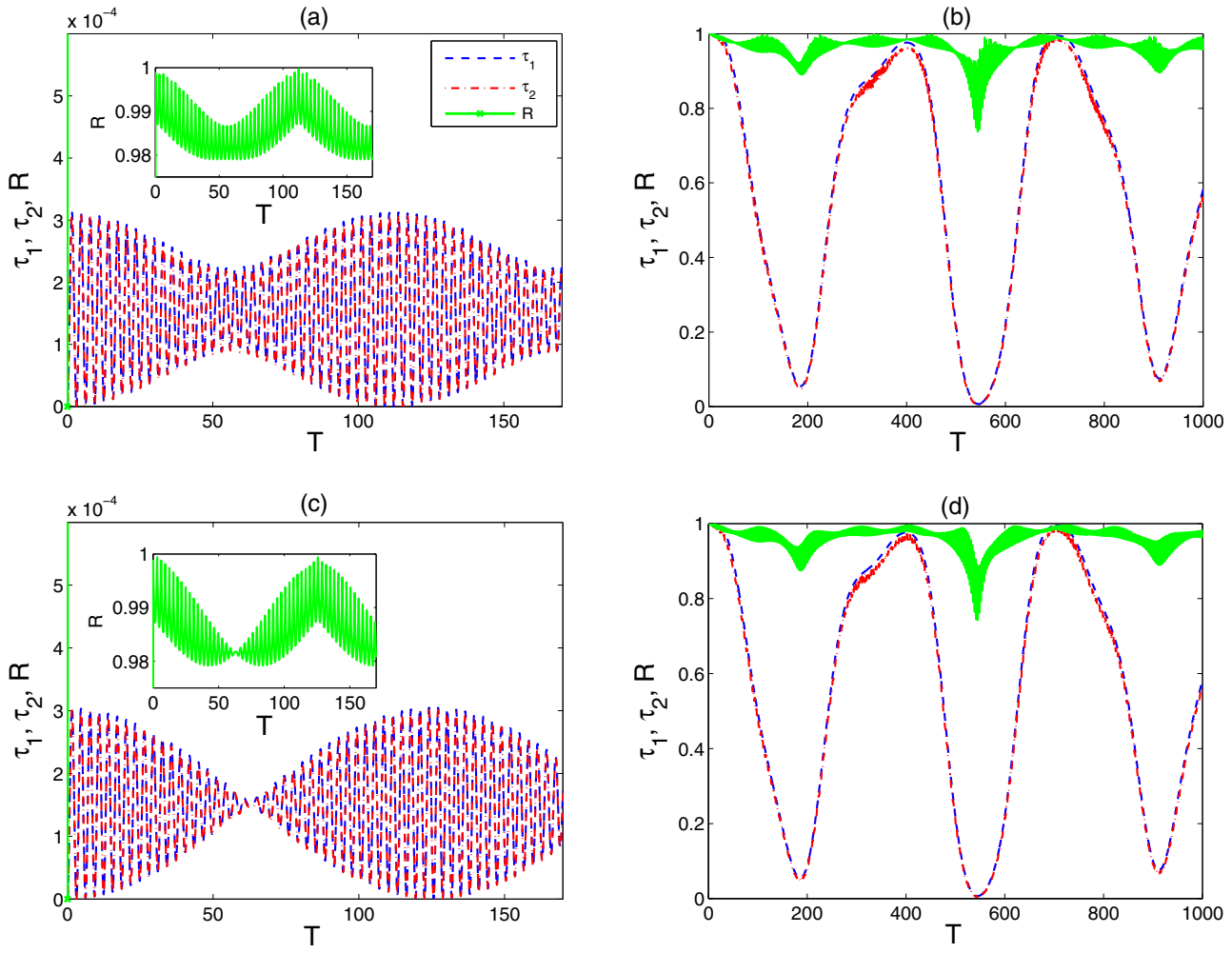

FIG. 4. Time evolution of the free XY system ($\Gamma = 0$) starting from an initial (a) disentangled state; (b) maximally entangled state; and the free XYZ system starting from an initial (c) disentangled state; (d) maximally entangled state, where $N = 5$. The legend is as shown in panel (a).

as shown in Fig. 2(a). As can be noticed, when the multipartite entanglement decreases significantly the contribution of the pairwise correlations becomes minimum. In Figs. 2(b) and 2(c) we plot the bipartite entanglements C_{12}, C_{13}, C_{14}, C_{15}, C_{16}, and C_{17}. They all show nonuniform oscillatory behavior, where interestingly the (nnn) entanglement C_{13} profile looks exactly like that of C_{17} but not like C_{16} as one may have expected for a closed boundary chain. The same applies to C_{14} which is exactly the same as C_{16} (not C_{15} as one would expect). This means that the maximum entanglement that was initially created between spins 1 and 2 is propagating through the chain in both directions starting from spins 1 and 2 as a single source. Comparing the results in Figs. 1 and 2, one can notice how the initial state causes a great deal of difference on the entanglement dynamics through the entire spin chain. Starting from a maximally entangled state leads to much higher amplitude of entanglement oscillation among all spins and much smaller frequency.

In Figs. 3(a) and 3(b) we consider the Ising chain again but with only five spins to examine the size effect, where we focus on the time evolution of τ_1, τ_2, and R. The oscillation of the system entanglement starting from a disentangled state is losing much of its beatlike character although the amplitude is almost the same as for $N = 7$ and the ratio R is closer to 1 with narrower range as shown in Fig. 3(a). The time evolution of the same system starting from an initial maximally entangled state is illustrated in Fig. 3(b). As one can see, the oscillation of the entanglements τ_1 and τ_2 become more uniform compared with the $N = 7$ case and also the range of R is narrower. In Figs. 3(c) and 3(d), we test the effect of removing the anisotropy (between X and Y) by considering the XX system. The initial state of the system is significantly affecting the system dynamics where the initial separable state, as shown in Fig. 3(c), causes the system to stay separable forever whereas the initial maximum entangled state, depicted in Fig. 3(d), leads to an oscillation, similar to what we have seen in Fig. 3(b) but with perfect coincidence between τ_1 and τ_2. Therefore removing the anisotropy from the system leads to an entanglement that is entirely due to pairwise correlations. The behavior of the partial anisotropic system, XY, is illustrated in Figs. 4(a) and 4(b), where it looks very similar to the Ising case but with a smaller range of variation of the ratio R. In Figs. 4(c) and 4(d) we test the effect of anisotropy not only in the X and Y directions but also in the Z direction

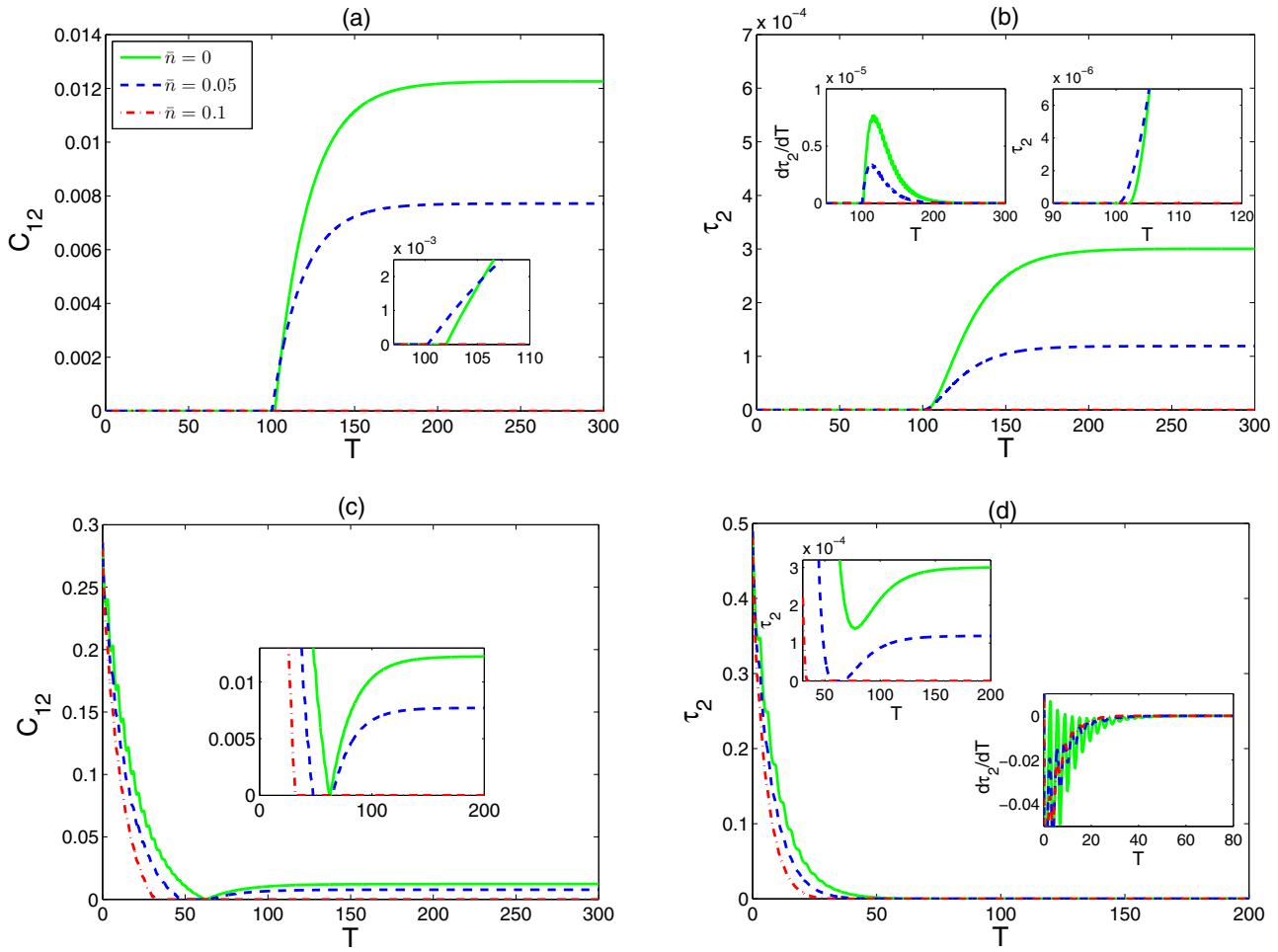

FIG. 5. Time evolution of C_{12} and τ_2 in the Ising system in presence of the environment ($\Gamma = 0.05$) starting from an initial disentangled state in (a) and (b) and an entangled W state in (c) and (d) respectively at different temperatures $\bar{n} = 0,\ 0.05$, and 0.1, where $N = 7$. The legend is as shown in panel (a).

by considering the XYZ system. It is clear that adding an interaction in the z direction is not changing the behavior of the system significantly compared with the XY model. The main change is the appearance of a node in the envelope of the oscillation in the initial separable state case. Obviously, the system size has a significant effect on the entanglement oscillation profile; when the system contains only two spins the entanglement oscillation is perfectly sinusoidal as is well known. Adding more spins makes every spin in the system interact and get entangled with more than one spin simultaneously, causing a nonuniformity of the entanglement oscillation, which increases with the system size.

B. Coupling to a thermal dissipative environment

In this section we study the dynamics of entanglement in different closed boundary Heisenberg spin chains, with different degrees of spatial anisotropy, coupled to a Lindblad environment at zero and finite temperatures, starting from different initial states. In this paper, we set up the system parameters such that $\omega = 1$, $\Gamma = J = 0.05\omega$, and the temperature parameter $0 \leqslant \bar{n} \leqslant 0.1(\sim 41$ mK), unless otherwise stated. We focus here on the time evolution of the nearest-neighbor bipartite entanglement between the two spins 1 and 2 as well as τ_2 between spin 1 and the rest of the chain, which gives a very good insight of how the overall bipartite entanglement and the beyond nearest-neighbor entanglement are behaving. We start with the Ising system, in Figs. 5(a) and 5(b), where we show the time evolution of C_{12} and τ_2 respectively starting from an initially separable state. As one can see, both C_{12} and τ_2 start with zero initial value and stay zero for some time before suddenly rising up and increasing monotonically to reach a steady-state value. To ensure that the final state is a sustainable steady state, we plot the first derivative of τ_2 versus time in the inner panel of Fig. 5(b), which shows a sudden peak at around $T \approx 100$ before decaying to zero $T \approx 240$. It is very clear how devastating is the temperature effect on the steady-state value of the entanglement, where having a value of $\bar{n} = 0.05$ reduces the steady-state value significantly compared with $\bar{n} = 0$ whereas $\bar{n} = 0.1$ keeps the system disentangled at all times. In Figs. 5(c) and 5(d), the system starts from an initial partially entangled state, the w state. As a result the entanglement C_{12} at zero temperature, shown in Fig. 5(c), starts with an initial nonzero value but decays with time until it vanishes but immediately revives again and increases monotonically reaching a steady state. As

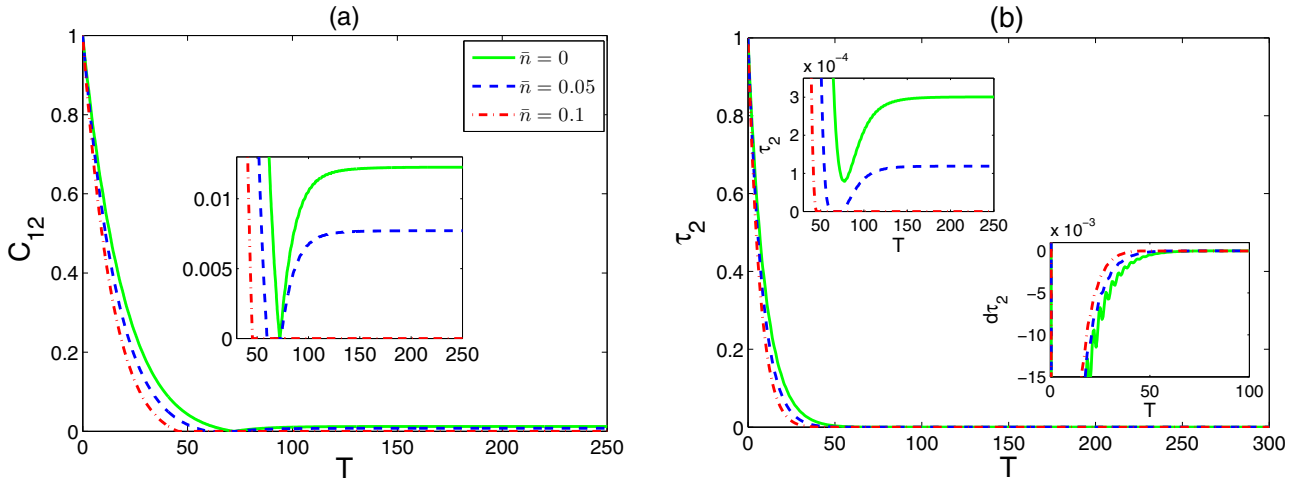

FIG. 6. Time evolution of (a) C_{12} and (b) τ_2 in the Ising system in presence of the environment ($\Gamma = 0.05$) starting from an initial maximally entangled state at different temperatures $\bar{n} = 0,\ 0.05$, and 0.1, where $N = 7$. The legend is as shown in panel (a).

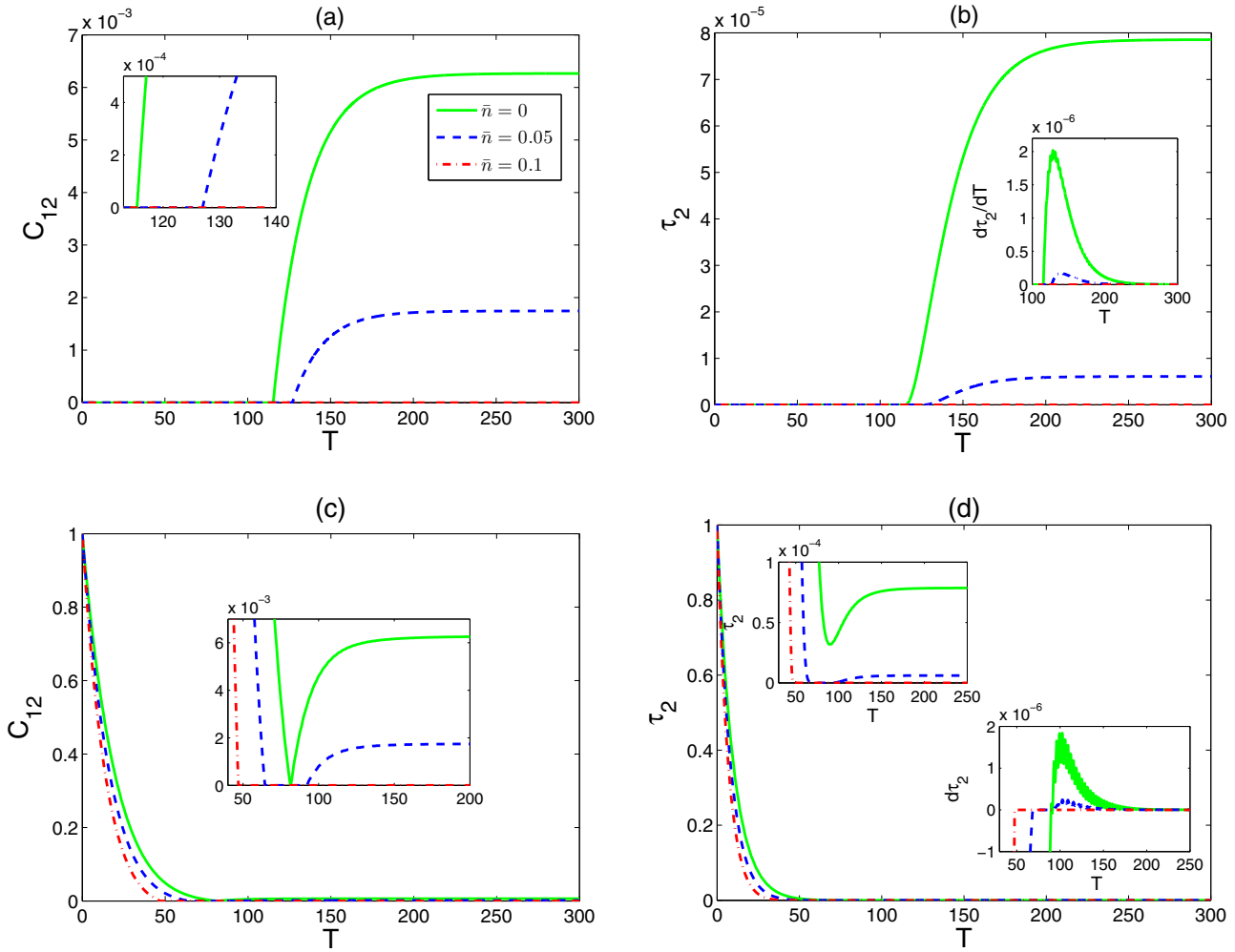

FIG. 7. Time evolution of C_{12} and τ_2 in the XYZ (or XY) system in presence of the environment ($\Gamma = 0.05$) starting from an initial disentangled state in (a) and (b) and a maximally entangled state in (c) and (d) at different temperatures $\bar{n} = 0,\ 0.05$, and 0.1, where $N = 7$. The legend is as shown in panel (a).

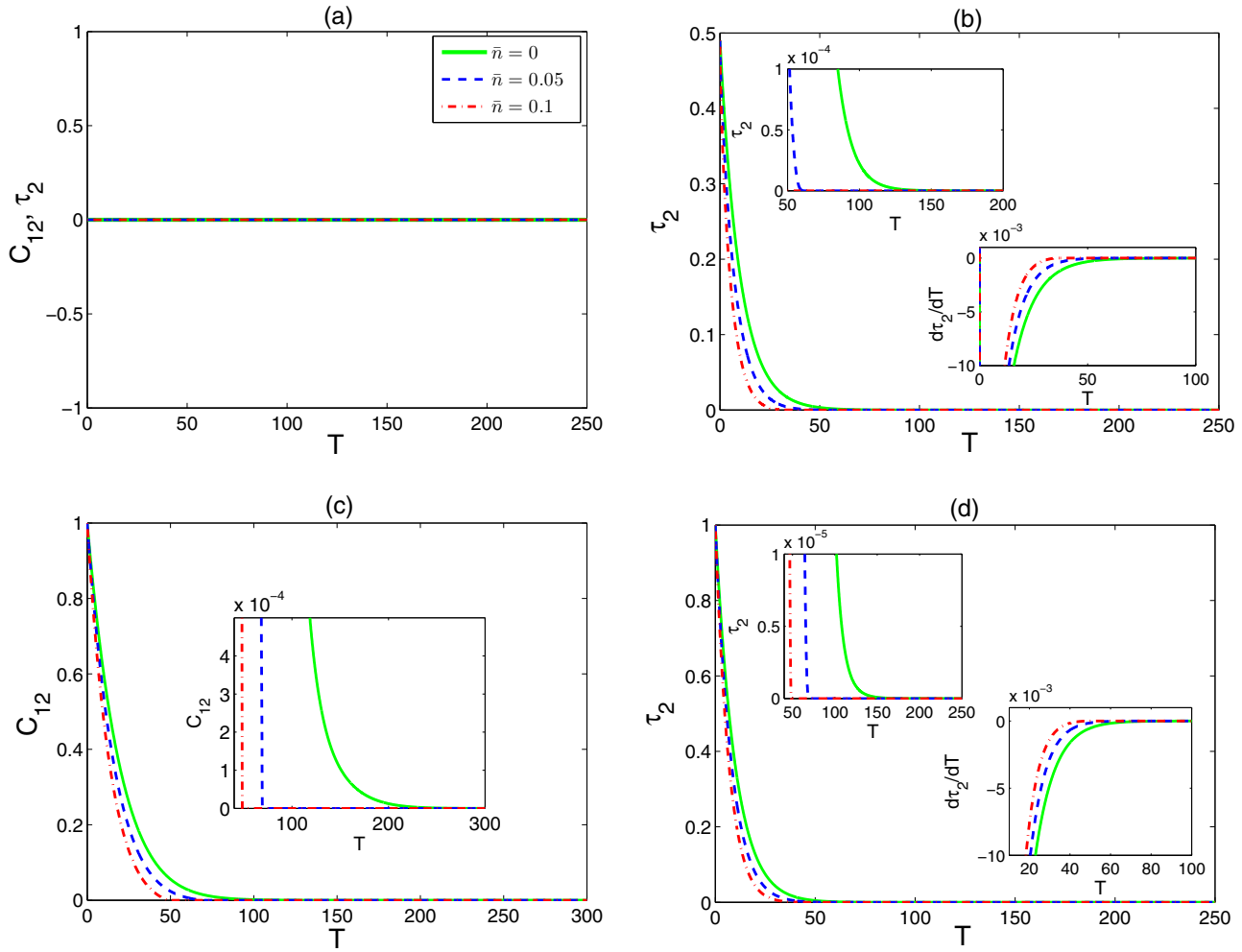

FIG. 8. Time evolution of C_{12} and τ_2 in the XX (XXX or XXZ) system in presence of environment ($\Gamma = 0.05$) starting from an initial (a) disentangled state; (b) entangled W state and maximally entangled state in (c) and (d) at different temperatures $\bar{n} = 0$, 0.05, and 0.1, where $N = 7$. The legend is as shown in panel (a).

the temperature increases, $\bar{n} = 0.05$, the entanglement death period increases and the steady-state value decreases. For higher temperature, $\bar{n} = 0.1$, the entanglement never revives again from its zero value. Interestingly, the behavior of τ_2, as illustrated in Fig. 5(d), is not exactly the same as C_{12}, where at zero temperature τ_2 decays as the system evolves, but never drops to zero, before rising up and reaching a steady state. This indicates that the beyond-nearest-neighbor entanglement sustains a nonzero value despite that the nearest-neighbor entanglement vanishes. The effect of the finite temperature on τ_2 is similar to that on C_{12} as can be concluded from the inner panels. The first derivative of τ_2 shows a rapid oscillation before reaching the zero value which is suppressed as the temperature is raised. In Fig. 6, we study the time evolution of the entanglement in the Ising system starting from an initial maximally entangled state. The overall dynamics of C_{12} and τ_2 is very close to what was observed when the system started from the W state except that the changes are sharper. More importantly, the steady-state values of C_{12} and τ_2 do not change in the three different cases of the Ising system, in Figs. 5 and 6, where different initial states of the system were considered. Nevertheless, the behavior of the first derivative of τ_2 varies considerably based on the initial amount of entanglement prepared in the system, becoming very smooth as the initial entanglement is increased as can be noticed in the inner panels in Figs. 5 and 6. During the transition process of τ_2 from zero to a steady-state value, the derivative lasts for different periods of time before reaching a zero value. The period is longest for an initial disentangled state. This stems from the fact that the system needs longer time and big rapid changes starting from a separable state to build up entanglement and reach a nonzero steady-state value. These needs are reduced as the initial amount of entanglement contained in the system is increased.

In Fig. 7, we consider the partially anisotropic XY system starting from two different initial states, separable in (a) and (b) and Maximally entangled in (c) and (d). The behavior of the entanglement C_{12} and τ_2 are similar to that of the Ising system with one main difference, which is a much smaller steady-state value for C_{12} and τ_2. Also we have tested the effect of the spin coupling in the z direction, by considering $0 < \delta \leqslant 1$, and particularly in the XYZ system. We did not find any noticeable change in either the dynamics of the system or the steady-state values as a result of this coupling for the set of parameter values that we are adopting here. The completely isotropic

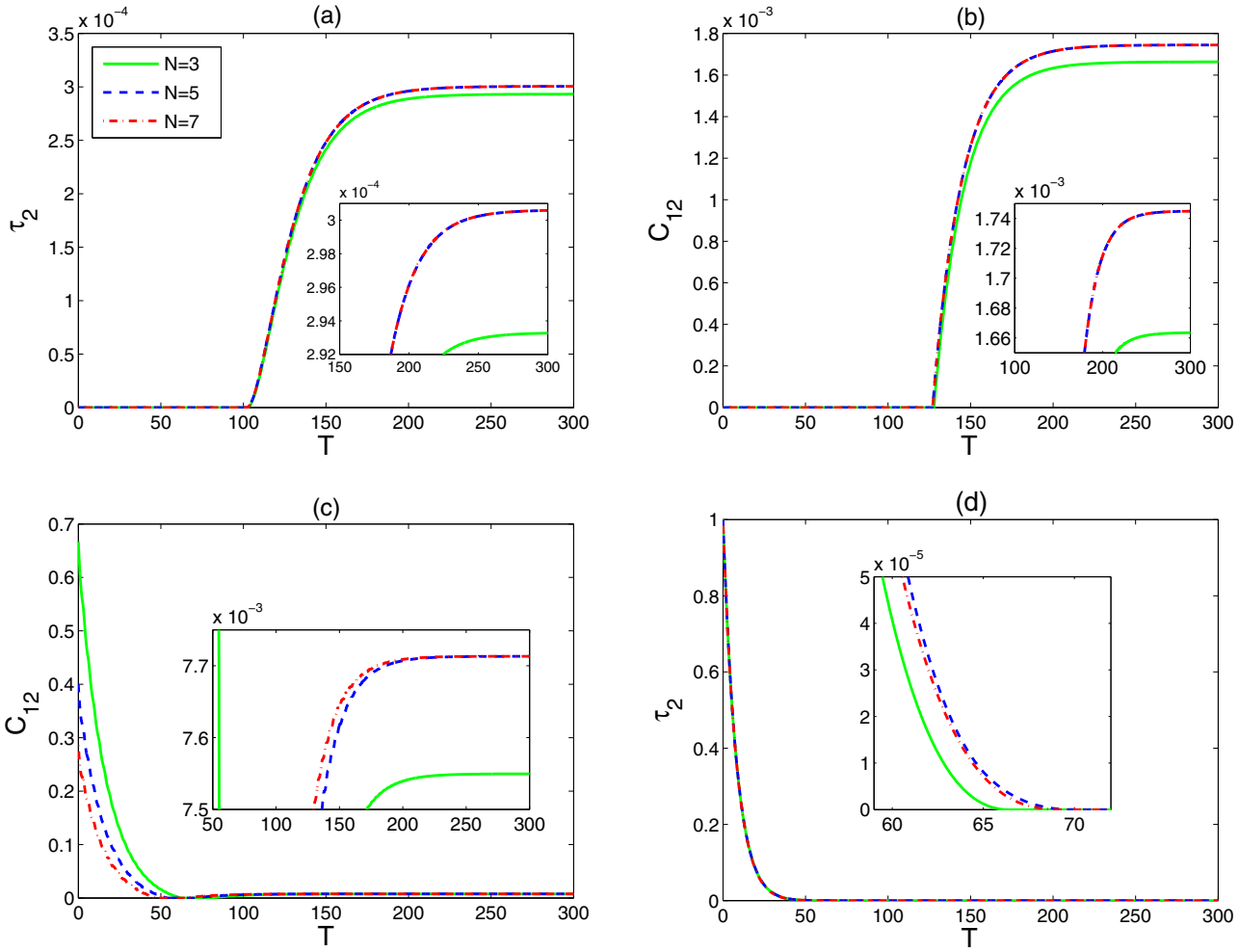

FIG. 9. Time evolution at different chain sizes ($N = 3$, 5, and 7) in presence of the environment ($\Gamma = 0.05$) of (a) τ_2 in the Ising system starting from an initial disentangled state at zero temperature; (b) C_{12} in the XYZ system starting from an initial disentangled state at temperature $\bar{n} = 0.05$; (c) C_{12} in the Ising system starting from an initial W-entangled state at temperature $\bar{n} = 0.05$; (d) τ_2 in the XX system starting from an initial maximally entangled state at zero temperature. The legend is as shown in panel (a).

XXX system is explored in Fig. 8, which shows a significantly different profile from the Ising and the XY systems. As one can see in Fig. 8(a), when the system starts from an initial separable state, both C_{12} and τ_2 start with and sustain a zero value as the system evolves in time at zero and finite temperatures. In Fig. 8(b), the time evolution of τ_2 is monitored in the XXX system starting from the W state. As can be seen, τ_2 starts with a value of about 0.5 and decays rapidly as the time elapses but ends up vanishing completely without any revival. As the temperature increases, the vanishing of entanglement becomes sharper and earlier in time as can be concluded from the inner panels in Fig. 8(b). A very similar behavior of C_{12} and τ_2 is observed as the XXX system starts from an initial maximally entangled state following the same dynamical behavior and ending up with a zero value, as illustrated in Figs. 8(c) and 8(d). Again testing the effect of spin coupling in the z direction, by studying the XX or XXZ systems, there were no noticeable changes, compared with the XXX system, either in the dynamics of the systems or the asymptotic values they reach. Clearly, the isotropic system reaches asymptotically a state with zero entanglement regardless of the initial amount of entanglement, as a result the behavior of the first derivative of τ_2 is very smooth across the transition period indicating that the system does not go through any critical changes as it loses its entanglement content, contrary to what has been observed in the anisotropic systems.

In Fig. 9, we examine the system size effect by studying the time evolution of the entanglement in chains with different total number of spins. In Fig. 9(a), we depict the time evolution of τ_2 for an Ising chain starting from an initial disentangled state at zero temperature for three different chain sizes ($N = 3$, 5, and 7). As can be noticed, the behavior of the entanglement dynamics converges very rapidly as N increases and the difference between the two cases of ($N = 5$ and 7) is quite small, which indicates a very small effect played by the system size as N becomes 5 or higher. The time evolution of C_{12} in an XYZ chain with different sizes starting from a disentangled state at finite temperature, $\bar{n} = 0.05$, is considered in Fig. 9(b). The behavior of C_{12} is very similar to that of τ_2, in Fig. 9(a), showing a rapid convergence and an almost same steady-state value for $N = 5$ and 7. In Fig. 9(c) we again examine the Ising system size at finite temperature but

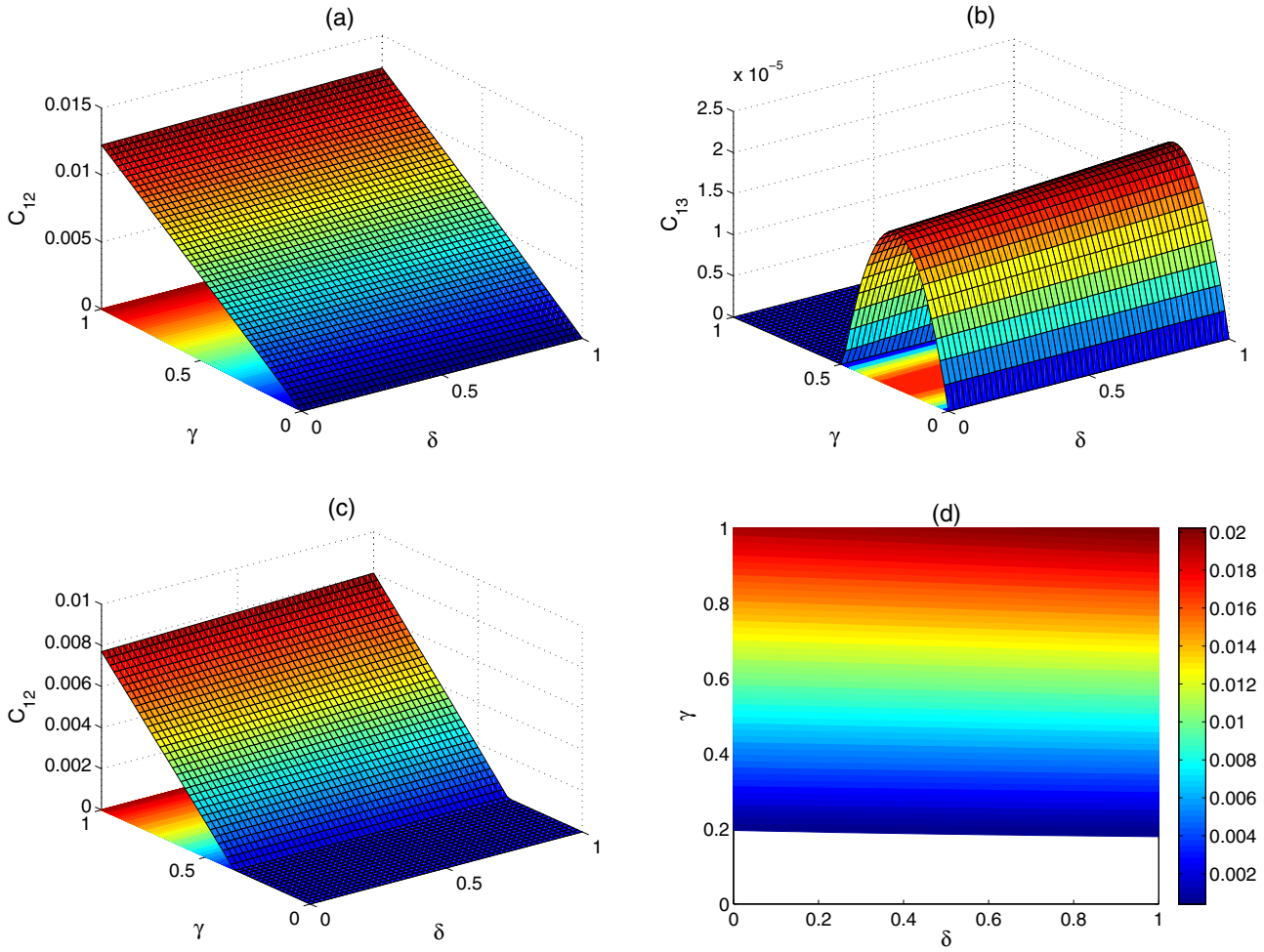

FIG. 10. The asymptotic behavior in the γ-δ space of the Heisenberg XYZ system in presence of the environment ($\Gamma = 0.05$), with $J = 0.05$ starting from any initial state (disentangled, entangled or maximally entangled) of (a) C_{12} at $\bar{n} = 0$, (b) C_{13} at $\bar{n} = 0$, (c) C_{12} at $\bar{n} = 0.05$, and (d) the contour plot of C_{12} at $\bar{n} = 0.05$ but for $J = 0.1$.

starting from partially entangled state whereas in Fig. 9(d) we depict τ_2 of the XX model starting from a maximally entangled state at zero temperature. The behavior of the entanglements C_{12} and τ_2, as illustrated Figs. 9(c) and 9(d), confirms our conclusion from Figs. 9(a) and 9(b). Interestingly, the system size in the presence of the environment is not playing the same important role as in the free system case. The environment does not only suppress the oscillation of the free system but also reduces significantly the effect of adding more spins to the system by diminishing the beyond-nearest-neighbor entanglements maintaining the same steady-state value.

In Fig. 10, the asymptotic (steady state) behavior of the entanglement in the γ-δ space of the XYZ Heisenberg five-spin chain is explored, where the steady-state value of C_{12} and C_{13}, at time $T = 300$, is depicted versus the anisotropic parameters γ and δ. The asymptotic value was found to be independent of the initial state of the system. Interestingly, the steady-state value of the entanglement, at zero temperature, shows a monotonic linear decay profile as the anisotropic parameter γ decreases and it vanishes at $\gamma = 0$ as shown in Fig. 10(a), whereas the parameter δ shows no effect on the steady-state value. The entanglement C_{13} shows a completely different behavior, as illustrated in Fig. 10(b), where it sustains a value of zero for $\gamma = 1$ up to $\gamma \approx 0.5$ before rising up to reach a maximum value at $\gamma \approx 0.25$, then it decays again until completely vanishing at $\gamma = 0$. Obviously, the robustness of the entanglement C_{13} against the decohering effect of the environment is not highest at maximum anisotropy, contrary to C_{12}. As the temperature increases, the entanglement C_{12} decreases but chains with higher γ (anisotropy) is more robust to thermal excitation whereas chains with low anisotropy lose their entanglement completely, as can be noticed in Fig. 10(c) where $\bar{n} = 0.05$, but as the temperature is raised further, the Heisenberg chains become fully disentangled regardless of their degree of anisotropy. As we concluded before and as can be noticed in Figs. 10(a)–10(c), the anisotropic parameter δ has no noticeable effect on the entanglement dynamics; the reason is the overwhelming magnetic field in the z direction compared with the component of the spin coupling J in the same direction. To clarify this point, in Fig. 10(d), we have applied a greater value of J, 0.1 instead of 0.05, and as can be seen in the contour plot of the entanglement C_{12} versus γ and δ, the entanglement steady-state value slightly increases

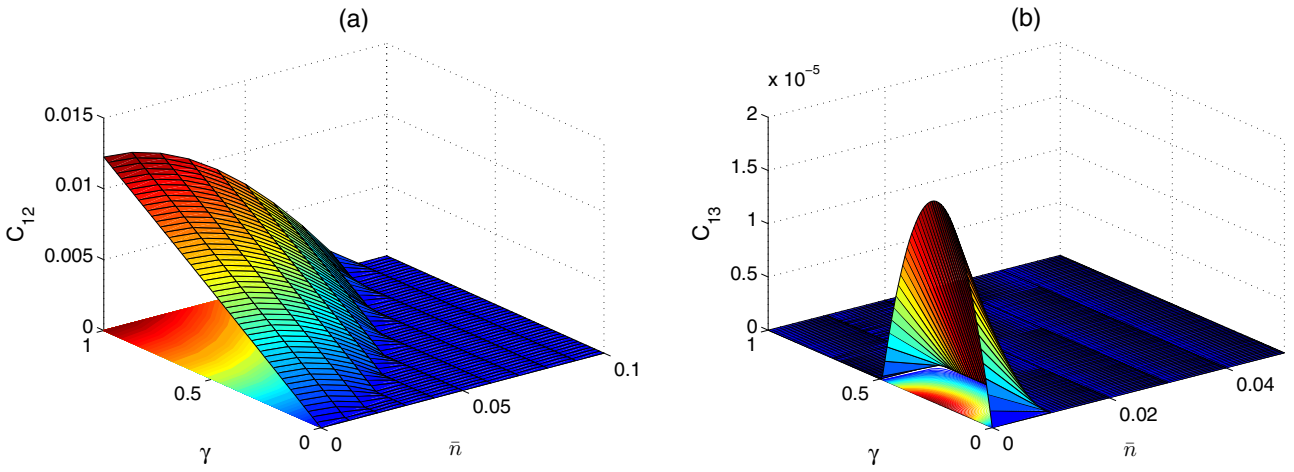

FIG. 11. The asymptotic behavior of C_{12} and C_{13} in the Heisenberg system in presence of the environment ($\Gamma = 0.05$) vs the anisotropy parameter γ and the temperature parameter $\bar{n}$ starting from any initial state (disentangled, entangled, or maximally entangled) and at any value of $0 \leqslant \delta \leqslant 1$.

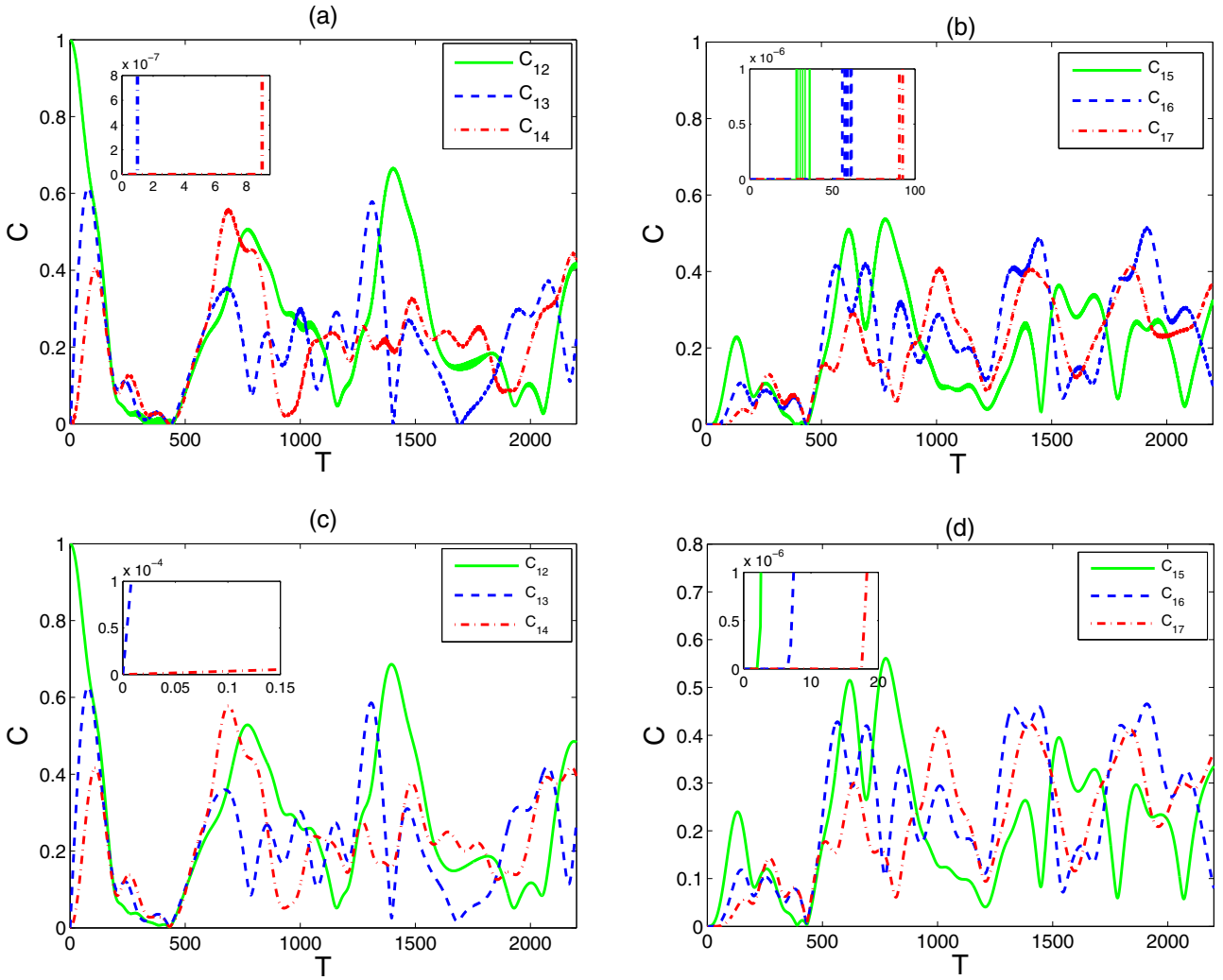

FIG. 12. The dynamics of the entanglements C_{12}, C_{13}, C_{14}, C_{15}, C_{16}, and C_{17} starting from a maximally entangled state in the free Ising system ($\Gamma = 0$) in (a) and (b) and the free XX system in (c) and (d) with open boundary condition, where $N = 7$. The inner panels illustrate the rise up of the entanglement from zero.

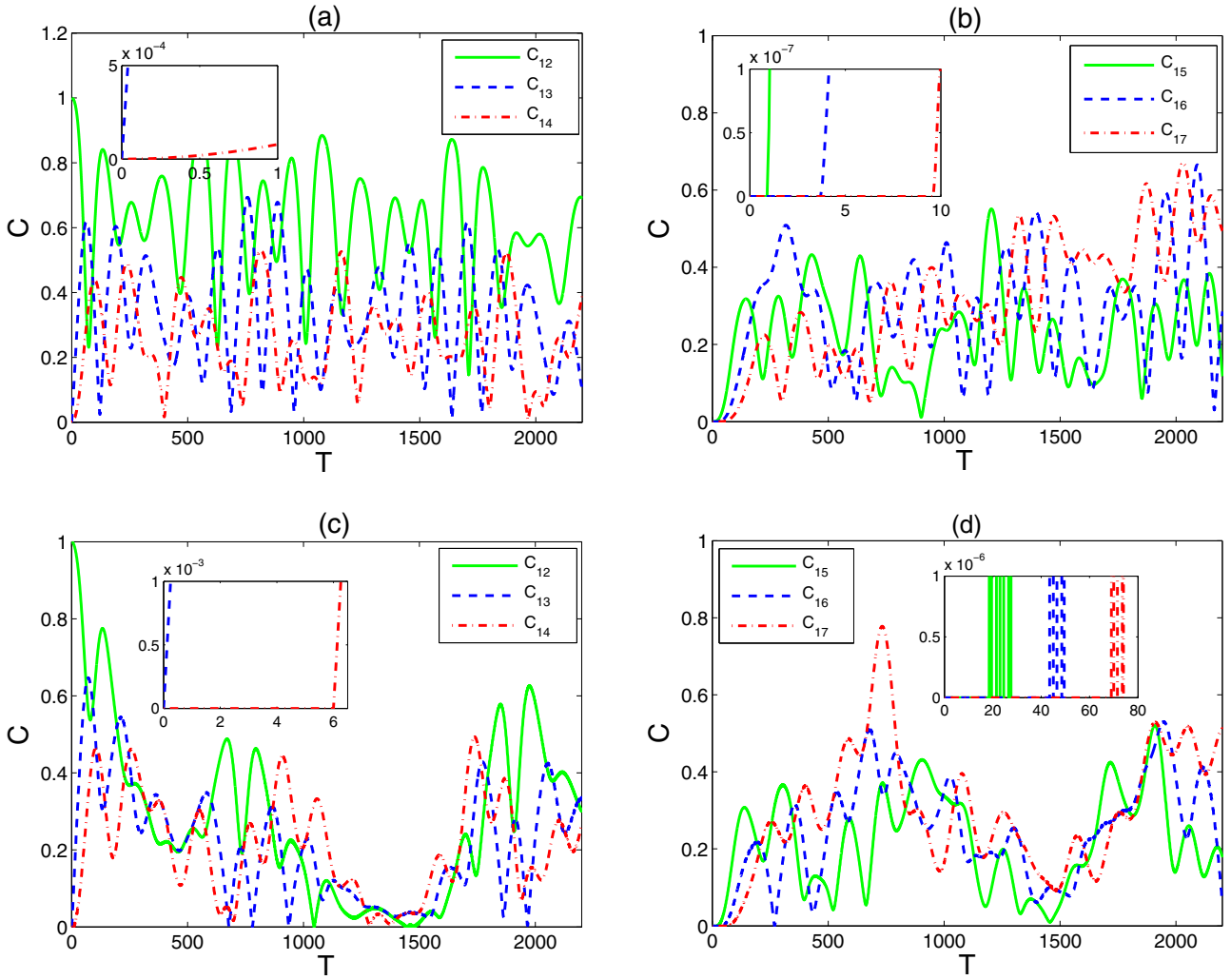

FIG. 13. The dynamics of the entanglements C_{12}, C_{13}, C_{14}, C_{15}, C_{16}, and C_{17} starting from a maximally entangled state of the free *XXZ* system ($\Gamma = 0$) in (a) and (b) and the free *XYZ* system in (c) and (d) with open boundary condition, where $N = 7$. The inner panels illustrate the rise up of the entanglement from zero.

as δ is increased, which means higher δ would enhance the value of the entanglement. To further investigate the effect of thermal excitations on the asymptotic steady state of the Heisenberg chains, we depict the asymptotic values of the entanglements C_{12} and C_{13} versus the anisotropy parameter γ and the temperature parameter $\bar{n}$ in Fig. 11. The results confirm our observations from the previous figure, where the (nn) entanglement C_{12} is more robust to thermal excitation in the completely anisotropic system and less as the degree of anisotropy decreases until it becomes very fragile in the isotropic system, as shown in Fig. 11(a). Also the (nnn) entanglement C_{13}, explored in Fig. 11(b), shows robustness for approximately $0 < \gamma \leqslant 0.5$ with its peak at $\gamma \approx 0.25$. This indicates that while the completely anisotropic system ($\gamma = 1$) enjoys a very robust nearest-neighbor entanglement, its beyond nearest-neighbor entanglement is not and vice versa for the partially anisotropic system ($0 < \gamma < 0.5$), if we ignore the role of the parameter δ. The entanglements C_{14} and C_{15} were found to show exactly the same behavior as C_{13} and C_{12} respectively as would be expected for a closed boundary spin chain.

IV. END TO END ENTANGLEMENT TRANSFER IN OPEN BOUNDARY SPIN CHAINS

A. Free system

The entanglement transfer through open boundary spin systems has been always the focus of interest as it plays an important role in implementing the different algorithms in quantum computing systems. In this section, we start by investigating the entanglement dynamics and transfer in one-dimensional free Heisenberg spin chains with open boundary condition. The system is initially prepared in a state with two spins (1 and 2) at one end of the chain maximally entangled with each other and are completely disentangled from the rest of the spins in the chain, which are also disentangled from each other. We start with the Ising seven-spin system, which is explored in Figs. 12(a) and 12(b). The (nn) entanglement C_{12} starts at $t = 0$ with a value of 1 but decays to zero before reviving and showing a nonuniform oscillatory behavior. The longer range entanglements C_{13}, C_{14}, C_{15}, C_{16}, and C_{17}, illustrated in Figs. 12(a) and 12(b), start with a zero value at $t = 0$ before rising up at later times; the longer the range

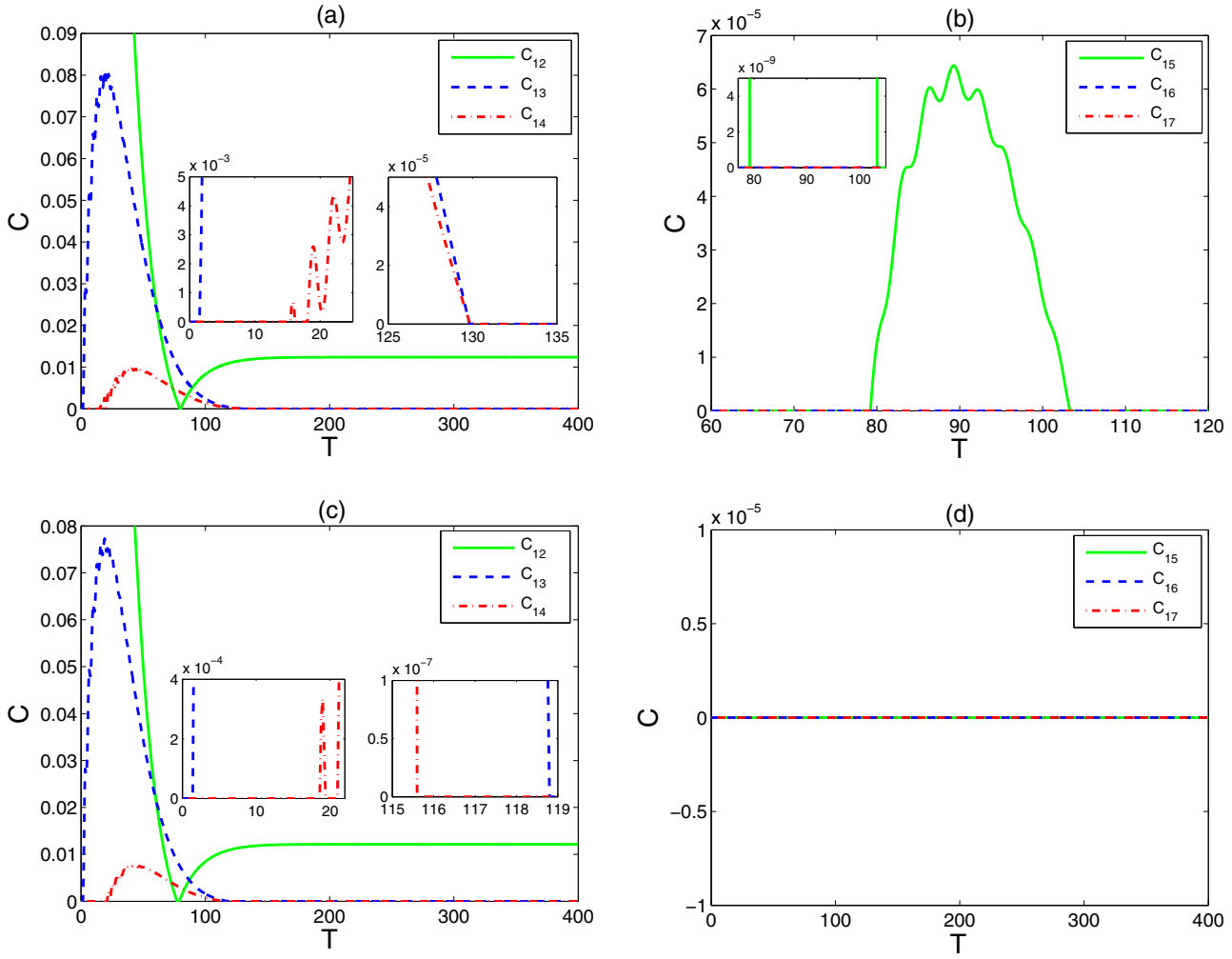

FIG. 14. The dynamics of the entanglements C_{12}, C_{13}, C_{14}, C_{15}, C_{16}, and C_{17} starting from a maximally entangled state in the Ising system in presence of the environment ($\Gamma = 0.05$) at $\bar{n} = 0$ in (a) and (b) and $\bar{n} = 0.01$ in (c) and (d), where $N = 7$. In (a) and (c), the left inner panels illustrate the rise up of entanglement while the right ones illustrate its death. In (b) the inner panel shows both of the rise up and death of entanglement.

of the entanglement is the longer it takes to rise up as shown in the inner panels of Figs. 12(a) and 12(b). In Figs. 12(c) and 12(d), we turn to the entanglement dynamics in the *XX* system, which shows one significant difference from what we have observed in the Ising system; the (nnn) entanglement C_{13} starts to rise up immediately at $t = 0$ but the other long-range entanglements are delayed, but not for as long as they were in the Ising system, as shown in the inner panels of the figure. Right after the different start all the entanglements, nearest neighbor and beyond, show very a close profile of oscillation to that of the Ising case. So the entanglement dynamics in these cases are asymptotically very close. To test the effect of the spin coupling in the z direction on the entanglement transfer dynamics, we explore the *XXZ* chain in Figs. 13(a) and 13(b) and the *XXZ* chain in Figs. 13(c) and 13(d). Clearly, there is a good resemblance between the rise up of the beyond-nearest-neighbor entanglement in the *XX* and *XXZ* systems but asymptotically they have different oscillation profile. On the other hand, the *XYZ* system has C_{13} rising up immediately from zero but the other longer range entanglements rise up much later compared with the previous cases with very strong oscillation and also show a different asymptotic oscillation profile. Comparing the entanglement dynamics and transfer through the open and closed boundary free spin chains with only two spins (1 and 2) initially maximally entanglement reveals interesting observations. In the Ising chain with closed boundary, illustrated in Fig. 1, the amplitude of the nearest-neighbor entanglement C_{12} is clearly higher than that of the beyond-nearest-neighbor entanglements C_{13} and C_{14} (which have the same exact behavior as C_{17} and C_{16} respectively as explained before). On the other hand, in the open free Ising chain the amplitude of C_{12} is close to that of the beyond-nearest-neighbor entanglements. This contrast is attributed to the fact that the initial source of the entanglement in the open chain is located at one end of the chain and propagates in one direction to the other end, whereas in the closed chain case the initial entanglement splits and propagates in two opposite directions at the same time, as we explained before.

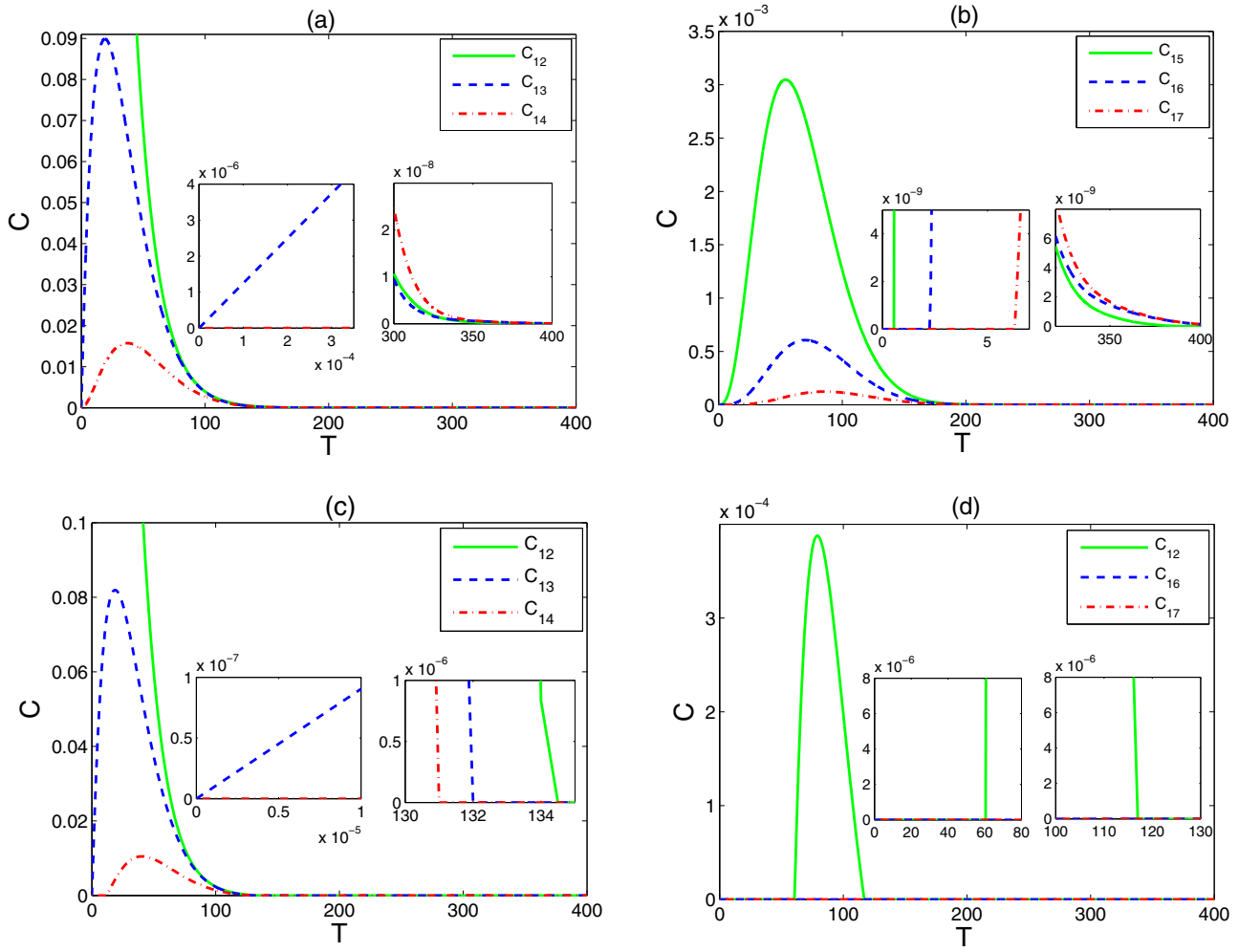

FIG. 15. The dynamics of the entanglements C_{12}, C_{13}, C_{14}, C_{15}, C_{16}, and C_{17} starting from a maximally entangled state in the XX system in presence of the environment ($\Gamma = 0.05$) at $\bar{n} = 0$ in (a) and (b) and $\bar{n} = 0.01$ in (c) and (d), where $N = 7$. The left inner panels illustrate the rise up of entanglement while the right ones illustrate its death.

B. Entanglement transfer in presence of the environment

Now we turn to examine the effect of the dissipative environment and thermal excitations on the entanglement transfer through the open boundary Heisenberg spin chains. We start with the Ising system at zero temperature in Figs. 14(a) and 14(b), where as can be noticed the (nn) entanglement C_{12} starts from a maximum value of 1 and decays very rapidly to 0 before reviving again to reach a steady-state value of about 0.0123. The (nnn) entanglement C_{13} is not created at $T = 0$ but a very short time later, $T \approx 1.5$, and rises up as shown in the left inner panel in Fig. 14(a); it reaches a maximum value, $C \approx 0.08$, before decaying again and vanishing at around $T = 130$ as shown in the right inner panel of Fig. 14(a). The (nnnn) entanglement C_{14} shows a very similar behavior to that of C_{13}, where it starts at a later time $T \approx 16$ with a strong oscillation reaching a maximum value of about 0.0045, then decaying and vanishing at about the same time as C_{13}, which is presented in the right inner panels of Fig. 14(a). The (nnnn) entanglement C_{15} starts at even latter time $T \approx 78$, as illustrated in Fig. 14(b), and increases to reach a maximum value before decaying and vanishing at $T \approx 104$. The entanglements beyond C_{15} are zero and never rise up. The effect of the finite temperature, $\bar{n} = 0.01$, on the Ising system is tested in Figs. 14(c) and 14(d). The overall behavior of the entanglements C_{12}, C_{13}, and C_{14} is very close to the zero-temperature case; the main changes are the reduction in the maximum values of the entanglements and the vanishing times of C_{13}, C_{14} become different from each other and earlier than before. The entanglement functions C_{15}, C_{16}, and C_{17} never rise up from zero as the temperature is raised as can be noticed in Fig. 14(d). Of course, as the temperature is raised further all the entanglements vanish.

The entanglement transfer in the XX spin chain is explored in Fig. 15. Contrary to the Ising case, at zero temperature, the (nnn) entanglement C_{13} starts to rise up immediately at $t = 0$ with no delay, as illustrated in Fig. 15(a) and the left inner panel, but the other far entanglements, C_{14}, C_{15}, and even C_{16} and C_{17} start up later on one after the other as shown in Figs. 15(a) and 15(b). But all entanglements decay asymptotically and vanish. As the temperature is raised, $\bar{n} = 0.01$, illustrated in Figs. 15(c) and 15(d), the (nnn) entanglement C_{13} still rises up at $t = 0$ whereas C_{14} and C_{15} are created later and C_{16} and C_{17} remain zero at all times. There is a significant change in the behavior of entanglement

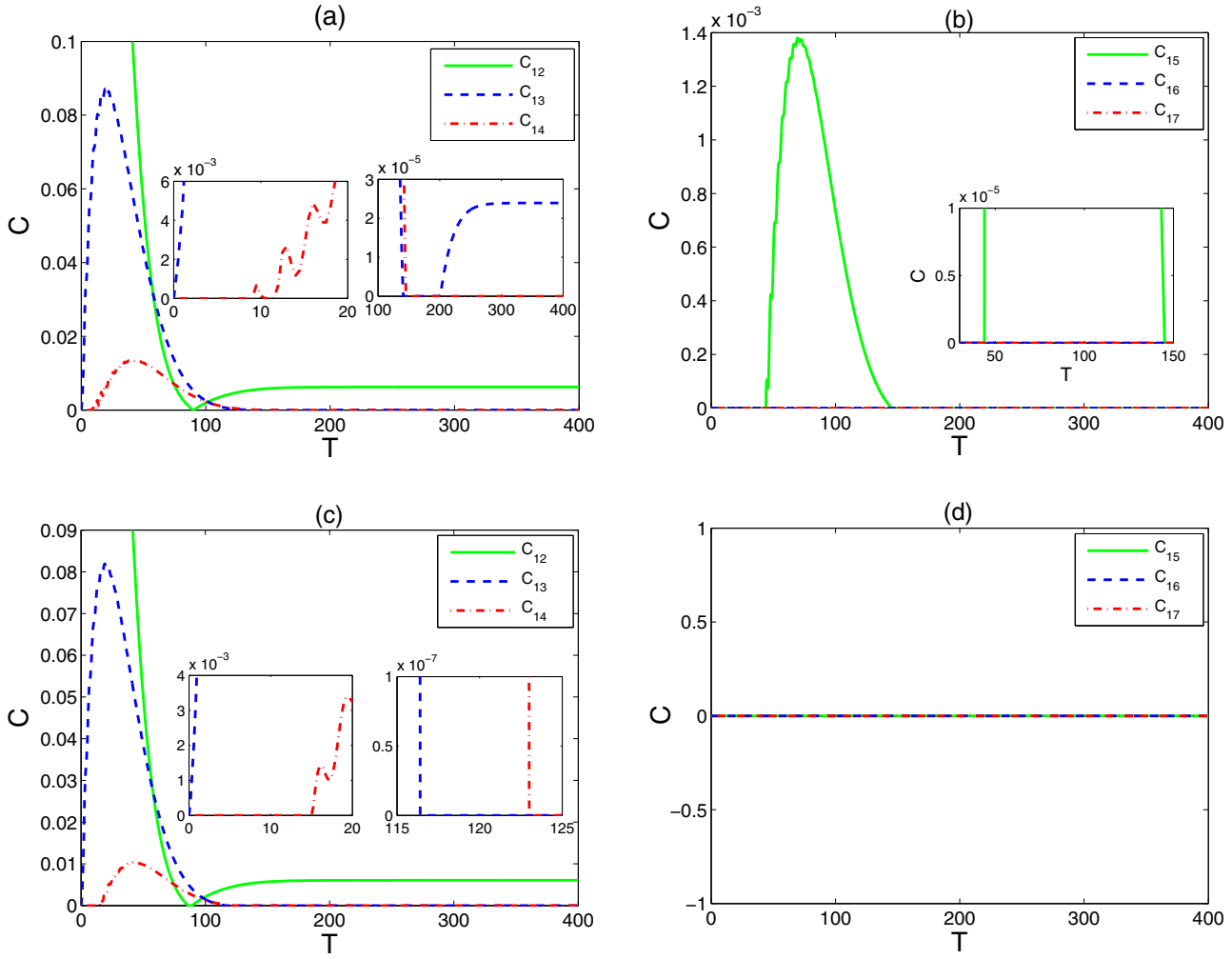

FIG. 16. The dynamics of the entanglements C_{12}, C_{13}, C_{14}, C_{15}, C_{16}, and C_{17} starting from a maximally entangled state in the *XYZ* system in presence of the environment at $\bar{n} = 0$ in (a) and (b) and $\bar{n} = 0.01$ in (c) and (d), where $N = 7$. In (a) and (c), the left inner panels illustrate the rise up of entanglement while the right ones illustrate its death. In (b) the inner panel shows both of the rise up and death of entanglement.

transfer in the *XYZ* system, depicted in Fig. 16, the (nnn) entanglement C_{13} at zero temperature reaches a steady state asymptotically, exactly like the (nn) entanglement C_{12}, as shown in Fig. 16(a). The steady state of C_{13} vanishes as the temperature is raised, $\bar{n} = 0.01$, contrary to that of C_{12}, which shows more robustness as illustrated in Fig. 16(c). The time evolution of the longer range entanglements C_{15}, C_{16}, and C_{17} is shown in Fig. 16(d), where they never rise up from zero. Clearly, the degrees of anisotropy not only play a major role in controlling the entanglement transfer dynamics in the Heisenberg spin chains but also affect the different pairwise entanglements in different ways. In order to further examine the effect of the anisotropy of the system at zero temperature, we plot the value of the entanglements C_{12}, C_{13}, C_{14}, and C_{15}, at $T = 300$ in the γ-δ space of Heisenberg spin system in Fig. 17, for $N = 5$. In general, the asymptotic behavior of the entanglements C_{12} and C_{13} looks very close to what has been observed in the closed boundary case except for a few small changes. As can be noticed in Fig. 17(a), the nn entanglement C_{12} decreases monotonically as γ decreases reaching zero at $\gamma = 0$ whereas the δ parameter has no noticeable effect on C_{12}. The (nnn) entanglement C_{13} shows a different behavior where it starts with a zero value, at $\gamma = 1$, and sustains this value up to $\gamma \approx 0.72$ (not $\gamma \approx 0.5$ as in the closed boundary case) before increasing to reach a maximum value at $\gamma \approx 0.42$ then it decreases again to reach a zero value at $\gamma = 0$, as illustrated in Fig. 17(b). There is a quite small effect on C_{13} due to the variation in the parameter δ, where the entanglement value increases monotonically (but very slightly) as δ increases. In Figs. 17(c) and 17(d), there are only nonzero values for C_{14} and C_{15} at $\gamma = 0$ and varies as δ is varied with a maximum value around $\delta = 0.5$ for C_{14} and $\delta = 0.75$ for C_{15}. In fact, the behavior of C_{12} and C_{13} do not change at later times so what is shown in Figs. 17(a) and 17(b) are their asymptotic steady-state values, which is not the case for C_{14} and C_{15} as they vanish at later time and never revive again. To test the entanglement robustness against thermal excitation at different degrees of anisotropy, we depict the values of entanglements C_{12}, C_{13}, C_{14}, and C_{15} at $T = 300$ versus both the anisotropic parameter γ and the temperature parameter $\bar{n}$ in Fig. 18. The resistance of the (nn) entanglement C_{12} to the thermal effects decreases as the degree of anisotropy of the system decreases as shown in Fig. 18(a) in a very similar fashion to the closed boundary case. On the other hand, the (nnn)

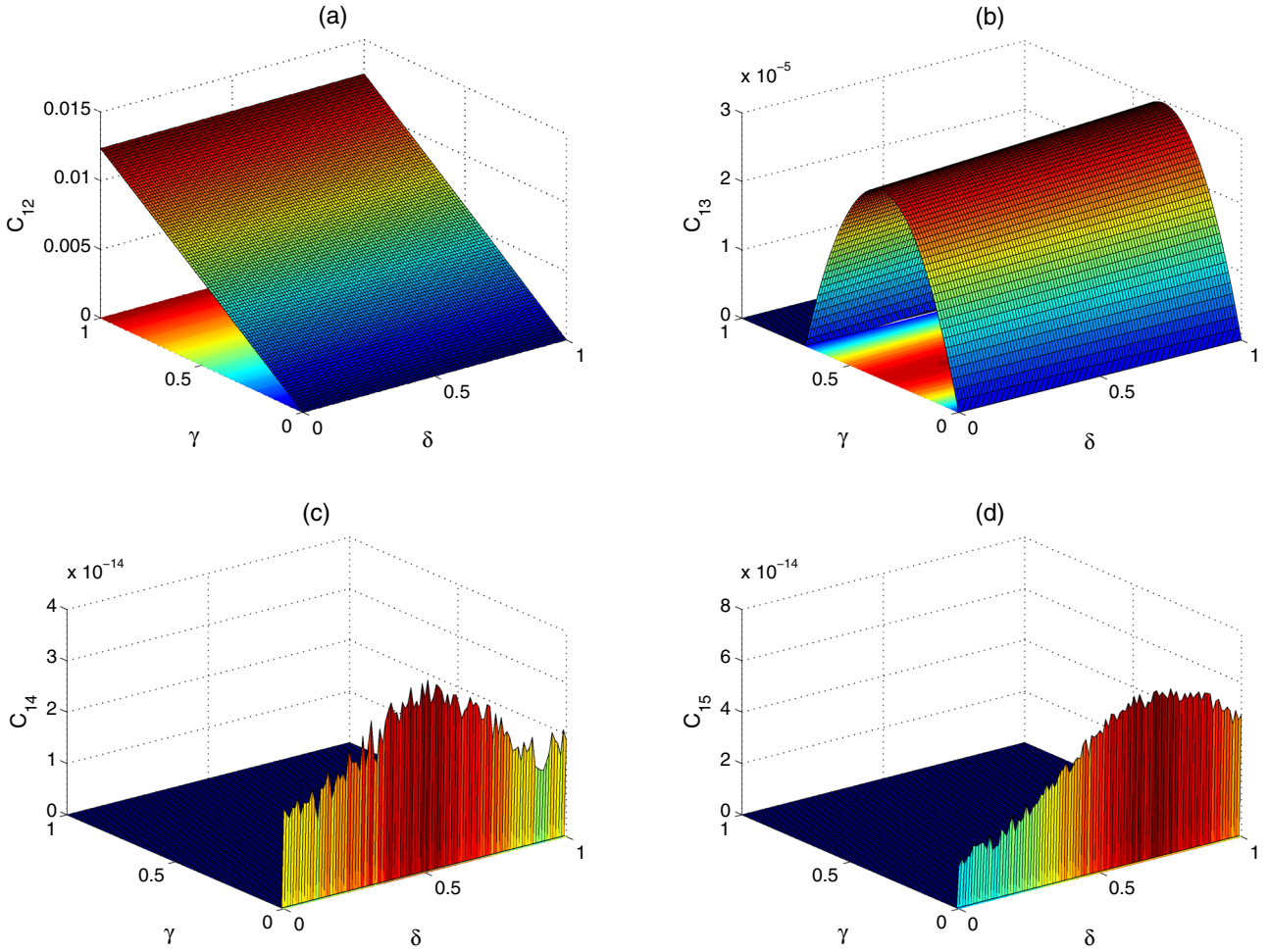

FIG. 17. The asymptotic behavior of (a) C_{12}, (b) C_{13}, and the value of (c) C_{14}, (d) C_{15} (at $T = 300$) in γ-δ space of the Heisenberg XYZ system in presence of the environment ($\Gamma = 0.05$) starting from any initial state (disentangled, entangled, or maximally entangled) at zero temperature, where $N = 5$.

entanglement C_{13} shows no resistance at high anisotropy values but rises up at $\gamma \approx 0.72$ reaching a maximum value at $\gamma \approx 0.42$ before vanishing again at $\gamma = 0$ as can be seen in Fig. 18(b), where it survives within $\bar{n} < 0.01$. The (nnnn) and (nnnnn) entanglements C_{14} and C_{15}, plotted in Figs. 18(c) and 18(d), exist only with a quite small value in the close vicinity of $\gamma = 0$ and $\bar{n} = 0$, which means these concurrences may survive only in the isotropic system very close to zero temperature. At later times, $T > 300$, the profiles of C_{12} and C_{13} do not change, whereas C_{14} and C_{15} vanish. Therefore, the quantum character and entanglement may persist in the Heisenberg spin chains even at nonzero temperature based mainly on the degree of spatial anisotropy in the system. The comparison of the entanglement dynamics and asymptotic behavior through the open boundary chain with that of the closed boundary chain in the presence of the environment shows that though the early dynamics of the system may differ, because of the way the entanglement is distributed and propagates, the asymptotic behavior in both cases has no remarkable difference. Therefore, the environment and temperature impact over a long period of time on both systems are the same.

V. CONCLUSIONS

We considered a finite one-dimensional Heisenberg spin chain with nearest-neighbor spin interaction under the influence of a dissipative Lindblad environment in the presence of an external magnetic field at finite temperature. We considered both cases of closed and open boundary spin chains with maximum number of seven spins. We presented an exact numerical solution for the Lindblad master equation of the system in Liouville space. We were mainly interested in investigating the effect of the spatial anisotropy, thermal excitations, system size, and initial-state entanglement content on the time evolution and asymptotic behavior of the nearest-neighbor, beyond-nearest-neighbor, and global pairwise entanglements. We fixed the values of the other parameters in the system such as the spin-spin coupling, the system-environment coupling and the magnetic-field strength in accordance with the Born-Markovian approximation.

In the closed boundary free Heisenberg spin chain, in the absence of the environments, the nearest-neighbor and beyond-nearest-neighbor entanglement as well as the one-tangle τ_1 and the global bipartite entanglement τ_2 were found to evolve in time in a nonuniform oscillatory form that changes

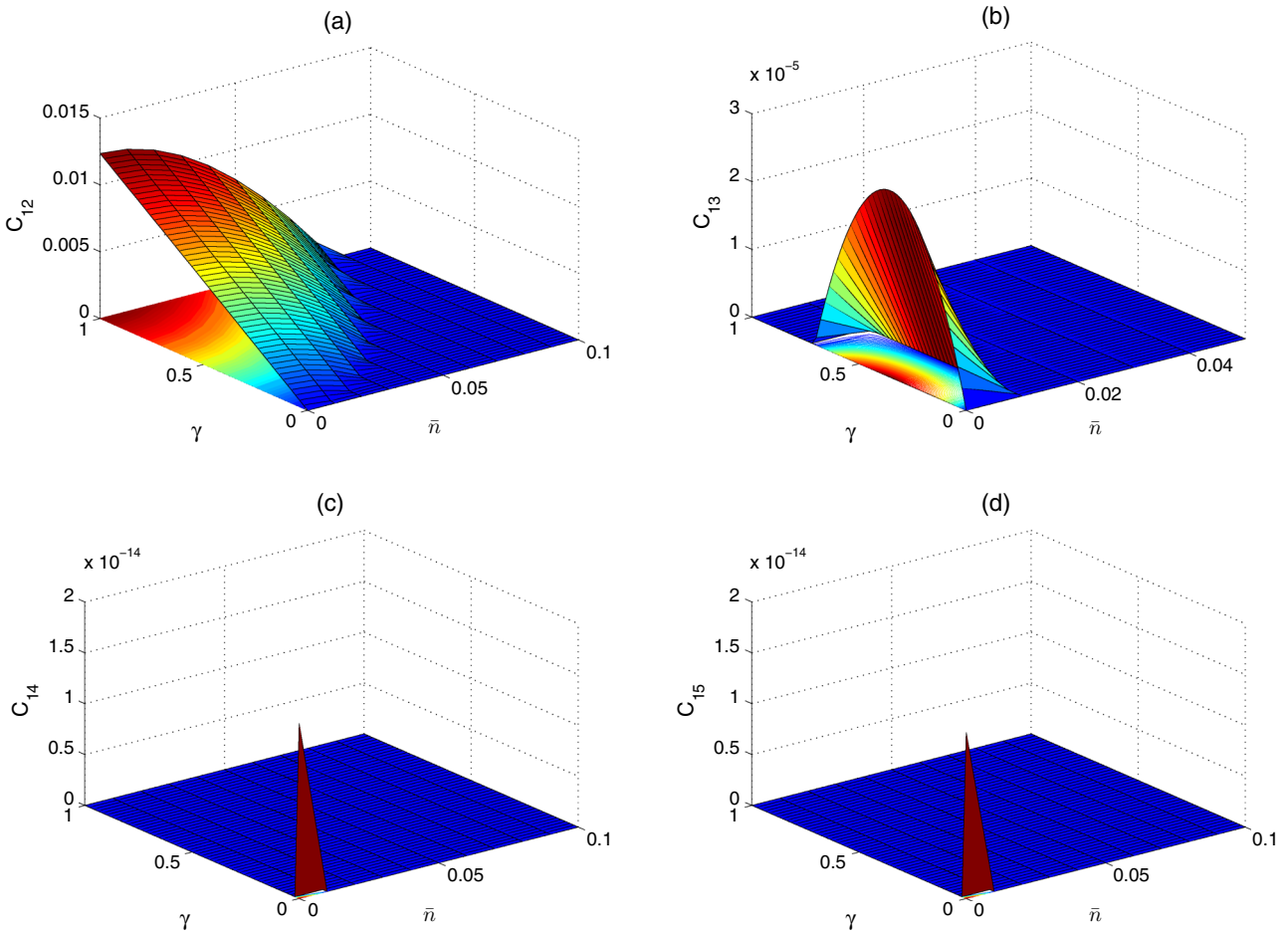

FIG. 18. The asymptotic behavior of (a) C_{12}, (b) C_{13}, and the value of (c) C_{14}, (d) C_{15} (at $T = 300$) in the Heisenberg XYZ system in presence of the environment ($\Gamma = 0.05$) vs the anisotropy parameter γ and the temperature parameter $\bar{n}$ starting from any initial state (disentangled, entangled, or maximally entangled) and for $\delta = 1$.

significantly depending on the initial state, system size, and the degree of spatial anisotropy. The oscillatory behavior of the entanglement in the spin chain is suppressed once the system is coupled to the environment. The time evolution of the entanglement at different ranges under the influence of the environment at zero temperature is substantially decided by the degree of spatial anisotropy in the spin-spin coupling in the x and y directions regardless of the entanglement content in the initial state. The anisotropy in the z direction may play an important role in enhancing the entanglements depending on the interplay with the magnetic field applied in the same direction, where strong magnetic field diminishes its effect. The anisotropy influences the entanglement at different ranges in different ways. Particularly, the asymptotic steady-state value of nearest-neighbor entanglement increases with higher anisotropy and vanishes for a completely isotropic system. In contrary, the next-nearest-neighbor entanglement is zero at complete anisotropy in x and y and reaches its maximum value at intermediate degree of anisotropy before vanishing again in the perfect isotropic case. The steady state of the nearest-neighbor and next-nearest-neighbor entanglements shows robustness against temperature up to very small nonzero temperature, which varies considerably depending on the degree of anisotropy. No significant size effect was observed for $N \geqslant 5$ in the presence of the environment. The end to end entanglement transfer through the chain with open boundaries was considered with a focus on both the early dynamics and the asymptotic behavior. We studied the entanglement transfer starting from a maximally entangled pair of spins at one end, which is initially disentangled from the rest of the mutually disentangled spins. The entanglement transfer time and speed through the chain vary depending on the degrees of anisotropy and the separation from the entangled pair for both of the free and environment-coupled systems. Higher anisotropy and temperature in the coupled system reduces the speed of the entanglement transfer considerably. The asymptotic behavior of the entanglements in the open boundary chain is also primarily decided by the degree of anisotropy and the temperature in a very similar pattern to the closed boundary chain case.

ACKNOWLEDGMENTS

This work was supported by the National Plan for Science, Technology and Innovation (MAARIFAH), King Abdulaziz City for Science and Technology, Saudi Arabia, Award No. 11-MAT1492-02.

[1] A. Peres, *Quantum Theory: Concepts and Methods* (Kluwer, Dordrecht, 1993).
[2] S. Sachdev, *Quantum Phase Transitions* (Cambridge University Press, Cambridge, England, 2001).
[3] M. Nielsen and I. Chuang, *Quantum Computation and Quantum Communication* (Cambridge University Press, Cambridge, England, 2000).
[4] W. H. Zurek, Phys. Today **44**(10), 36 (1991).
[5] D. Bacon, J. Kempe, D. A. Lidar, and K. B. Whaley, Phys. Rev. Lett. **85**, 1758 (2000).
[6] D. Loss and D. P. DiVincenzo, Phys. Rev. A **57**, 120 (1998).
[7] G. Burkard, D. Loss, and D. P. DiVincenzo, Phys. Rev. B **59**, 2070 (1999).
[8] A. Imamoglu, D. D. Awschalom, G. Burkard, D. P. DiVincenzo, D. Loss, A. Sherwin, and A. Small, Phys. Rev. Lett. **83**, 4204 (1999).
[9] B. E. Kane, Nature (London) **393**, 133 (1998).
[10] R. R. Ernst, G. Bodenhausen, and A. Wokaun, *Principles of Nuclear Magnetic Resonance in One and Two Dimensions* (Clarendon, Oxford, 1988).
[11] A. S. Sorensen and K. Molmer, Phys. Rev. Lett. **86**, 4431 (2001).
[12] W. M. Liu, W. B. Fan, W. M. Zheng, J. Q. Liang, and S. T. Chui, Phys. Rev. Lett. **88**, 170408 (2002).
[13] R. Vrijen, E. Yablonovitch, K. Wang, H. W. Jiang, A. Balandin, V. Roychowdhury, T. Mor, and D. DiVincenzo, Phys. Rev. A **62**, 012306 (2000).
[14] R. Heule, C. Bruder, D. Burgarth, and M. V. Stojanovic, Eur. Phys. J. D **63**, 41 (2011).
[15] G. Sadiek, B. Alkurtass, and O. Aldossary, Phys. Rev. A **82**, 052337 (2010).
[16] E. Barouch, Phys. Rev. A **2**, 1075 (1970).
[17] A. Sen(De), U. Sen, and M. Lewenstein, Phys. Rev. A **70**, 060304 (2004).
[18] Z. Huang and S. Kais, Phys. Rev. A **73**, 022339 (2006).
[19] E. Lieb, T. Schultz, and D. Mattis, Ann. Phys. **16**, 407 (1961).
[20] Q. Xu, S. Kais, M. Naumov, and A. Sameh, Phys. Rev. A **81**, 022324 (2010).
[21] Q. Xu, G. Sadiek, and S. Kais, Phys. Rev. A **83**, 062312 (2011).
[22] G. Sadiek and S. Kais, J. Phys. B **46**, 245501 (2013).
[23] J. Wang, H. Batelaan, J. Podany, and A. F. Starace, J. Phys. B **39**, 4343 (2006).
[24] A. Abliz, H. J. Gao, X. C. Xie, Y. S. Wu, and W. M. Liu, Phys. Rev. A **74**, 052105 (2006).
[25] Y. Dubi and M. DiVentra, Phys. Rev. A **79**, 012328 (2009).
[26] M. Hein, W. Dür, and H. J. Briegel, Phys. Rev. A **71**, 032350 (2005).
[27] D. I. Tsomokos, M. J. Hartmann, S. F. Huelga, and M. B. Plenio, New J. Phys. **9**, 79 (2007).
[28] N. Buric, Phys. Rev. A **77**, 012321 (2008).
[29] M. L. Hu and X. Q. Xi, Opt. Commun. **282**, 4819 (2009).
[30] M. L. Hu, X. Q. Xi, and H. L. Lian, Physica B: Condens. Matter **404**, 3499 (2009).
[31] N. Buric and B. L. Lindén, Phys. Lett. **A373**, 1531 (2009).
[32] N. Pumulo, I. Sinayskiy, and F. Petruccione, Phys. Lett. **A375**, 3157 (2011).
[33] X.-X. Zhang, A.-P. Zhang, J. Zhang, and J.-X. Wang, Mod. Phys. Lett. B **27**, 1350078 (2013).
[34] A. Lakshminarayan, Phys. Rev. E **64**, 036207 (2001).
[35] D. Petrosyan, G. M. Nikolopoulos, and P. Lambropoulos, Phys. Rev. A **81**, 042307 (2010).
[36] R. Ronke, T. P. Spiller, and I. D'Amico, Phys. Rev. A **83**, 012325 (2011).
[37] B. Alkurtass, H. Wichterich, and S. Bose, Phys. Rev. A **88**, 062325 (2013).
[38] N. Wu, A. Nanduri, and H. Rabitz, Phys. Rev. A **89**, 062105 (2014).
[39] G. Lindblad, Commun. Math. Phys. **48**, 119 (1976).
[40] H. P. Breuer and F. Petruccione, *The Theory of Open Quantum Systems* (Oxford University Press, Oxford, 2002).
[41] F. Mintert, A. R. R. Carvalho, M. Kus, and A. Buchleitner, Phys. Rep. **415**, 207 (2005).
[42] W. K. Wootters, Phys. Rev. Lett. **80**, 2245 (1998).
[43] V. Coffman, J. Kundu, and W. K. Wootters, Phys. Rev. A **61**, 052306 (2000).
[44] L. Amico, A. Osterloh, F. Plastina, R. Fazio, and G. M. Palma, Phys. Rev. A **69**, 022304 (2004).
[45] T. Roscilde, P. Verrucchi, A. Fubini, S. Haas, and V. Tognetti, Phys. Rev. Lett. **93**, 167203 (2004).